



## Chemical characterization of organic vapors from wood, straw, cow dung, and coal burning

Tiantian Wang<sup>1</sup>, Jun Zhang<sup>1</sup>, Houssni Lamkaddam<sup>1</sup>, Kun Li<sup>1,a</sup>, Ka Yuen Cheung<sup>1</sup>, Lisa Kattner<sup>1</sup>, Erlend Gammelsæter<sup>1,b</sup>, Michael Bauer<sup>1</sup>, Zachary C. J. Decker<sup>1,c,d</sup>, Deepika Bhattu<sup>2</sup>, Rujin Huang<sup>3</sup>, Rob L. Modini<sup>1</sup>, Jay G. Slowik<sup>1</sup>, Imad El Haddad<sup>1</sup>, Andre S. H. Prevot<sup>1</sup>, and David M. Bell<sup>1</sup>

<sup>1</sup>PSI Center for Energy and Environmental Sciences, Paul Scherrer Institute, 5232 Villigen, Switzerland

<sup>2</sup>Department of Civil and Infrastructure Engineering, Indian Institute of Technology Jodhpur, 342037, India

<sup>3</sup>Institute of Earth Environment, Chinese Academy of Sciences, Xian 710061, China

<sup>a</sup>now at: Environmental Research Institute, Shandong University, Qingdao, 266237, China

<sup>b</sup>now at: Department of Chemistry, Norwegian University of Science and Technology, Trondheim, 7491, Norway

<sup>c</sup>now at: NOAA Chemical Sciences Laboratory (CSL), Boulder, CO 80305, USA

<sup>d</sup>now at: Cooperative Institute for Research in Environmental Sciences, University of Colorado Boulder, Boulder, CO 80309, USA

**Correspondence:** Andre S. H. Prevot (andre.prevot@psi.ch) and David M. Bell (david.bell@psi.ch)

Received: 26 April 2024 – Discussion started: 2 May 2024

Revised: 23 November 2024 – Accepted: 19 December 2024 – Published: 3 March 2025

**Abstract.** Solid fuel (SF) combustions, including coal and biomass, are important sources of pollutants in the particle and gas phase and therefore have significant implications for air quality, climate, and human health. In this study, we systematically examined gas-phase emissions, using the Vocus proton-transfer-reaction time-of-flight (PTR-TOF) mass spectrometer, from a variety of solid fuels, including beech logs, spruce/pine logs, spruce/pine branches and needles, straw, cow dung, and coal. The average emission factors (EFs) for organic vapors ranged from 4.8 to 74.2 g kg<sup>-1</sup>, depending on the combustion phases and solid fuel types. Despite slight differences in modified combustion efficiency (MCE) for some experiments, increasing EFs for organic vapors were observed with lower MCE. The relative contribution of different classes showed large similarities between the combustion phases in beech logs stove burning, relative to the large change in EFs observed. The C<sub>x</sub>H<sub>y</sub>O<sub>z</sub> family is the most abundant group of the organic vapor emitted from all SF combustion. However, among these SF combustions, a greater contribution of nitrogen-containing species and C<sub>x</sub>H<sub>y</sub> families (related to polycyclic aromatic hydrocarbons) is observed in the organic vapors from cow dung burning and coal burning, respectively. Intermediate-volatility organic compounds (IVOCs) constituted a significant fraction of emissions in solid fuel combustion, ranging from 12.6% to 39.3%. This was particularly notable in the combustion of spruce/pine branches and needles (39.3%) and coal (31.1%). Using the Mann–Whitney *U* test on the studied fuels, we identified specific potential new markers for these fuels based on the Vocus measurements. The product from pyrolysis of coniferyl-type lignin and the extract of cedar pine needle were identified as markers in the open burning of spruce/pine branches and needles (e.g., C<sub>10</sub>H<sub>14</sub>O<sub>2</sub>, C<sub>11</sub>H<sub>14</sub>O<sub>2</sub>, C<sub>10</sub>H<sub>10</sub>O<sub>2</sub>). The product (C<sub>9</sub>H<sub>12</sub>O) from the pyrolysis of beech lignin was identified as the potential new marker for beech log stove burning. Many series of nitrogen-containing homologues (e.g., C<sub>10</sub>H<sub>11–21</sub>NO, C<sub>12</sub>H<sub>11–21</sub>N, C<sub>11</sub>H<sub>11–23</sub>NO, and C<sub>15</sub>H<sub>15–31</sub>N) and nitrogen-containing species (e.g., acetonitrile, acrylonitrile, propanenitrile, methylpentanenitrile) were specifically identified in cow dung burning emissions. Polycyclic aromatic hydrocarbons (PAHs) with 9–12 carbons were identified with significantly higher abundance from coal burning compared to emissions from other studied fuels. The composition of these organic vapors reflects the burned solid fuel types and can help constrain emissions of solid fuel burning in regional models.

## 1 Introduction

Solid fuels (SFs), including coal and biomass, are a primary source of domestic heating worldwide (Tao et al., 2018; Oberschelp et al., 2019; Wu et al., 2022). In developing regions, such as India, more than 80 % of rural households use biomass as cooking fuel (Balakrishnan et al., 2011). Firewood is mainly used for rural households, followed by crop residues and cow dung “cakes”, which are made of a mixture of dried cow dung and crop residues (Loebel Roson et al., 2021; Chandramouli and General, 2011). In Europe, fireplaces and woodstoves are used for domestic heating in winter and have considerable impacts on air quality, resulting in intense “smog” events (Kalogridis et al., 2018; Fourtziou et al., 2017; Bailey et al., 2019; Font et al., 2022). China is the largest producer and consumer of coal in the world. In China and some eastern European countries like Poland, coal is widely used for domestic purposes, such as heating and cooking of households, due to its cost-effectiveness and easy accessibility (Guo et al., 2021; Stala-Szlugaj, 2018). The combustion of these solid fuels has been recognized as the main source of anthropogenic emission of atmospheric pollutants that elicit adverse effects on air quality and human health (Wu et al., 2022; Zhang and Smith, 2007).

Wildfires or bushfires have become more frequent in many regions due to heat waves and drought (Weber and Yadav, 2020; Williams et al., 2013). SF combustion, including wildfires, is a major source of organic vapors to the atmosphere, emitting hundreds to thousands of different organic gas-phase species (Hatch et al., 2019; Koss et al., 2018; Permar et al., 2021). Once emitted, evaporated vapors or freshly emitted burning organic vapors will oxidize to produce oxygenated organic vapors with a broad volatility range. These organic vapors with sufficiently low volatility will nucleate or condense onto pre-existing aerosols to form secondary organic aerosols (SOAs) (Kumar et al., 2023).

The identification of potential markers for each emission source will be highly valuable in evaluating SOA formation potential and ambient source contributions. Liu et al. (2008) identified potential volatile organic markers for different emission sources (e.g., biomass burning (BB), mobile sources, and painting). Nevertheless, these commonly used potential markers are well established, yet, due to their presence in more than one type of biomass fuel, distinguishing between different biomass burning sources presents challenges. Since 2009, there have been many advancements in the gas-phase measurements of SF, which include lab studies (Bruns et al., 2017; Bruns et al., 2016; Bhattu et al., 2019) and large field campaigns (e.g., WE-CAN aircraft measurements, FIREX-AQ campaign) (Permar et al., 2021; Jin et al., 2023; Majluf et al., 2022). However, efforts towards understanding SOA formation in burning plumes have been hindered by limited identification and quantification of organic

vapors emitted by fires, especially intermediate-volatility organic compounds (IVOCs) (Akagi et al., 2011). Laboratory and field campaigns suggest that intermediate-volatility organic compounds are important precursors of SOA. Grieshop et al. (2009) demonstrated that traditional SOA precursors account for less than 20 % of the observed SOA formed from residential wood combustion emissions, while IVOCs can contribute approximately 70 % of the formed SOA (Li et al., 2024), which highlights the urgent need for more research on IVOCs from BB emissions. Adding an IVOC emission inventory to an air quality model can significantly narrow the gap between the estimated and measured SOA concentrations (Li et al., 2024; Hodzic et al., 2010; Zhao et al., 2016; Robinson et al., 2007).

Offline sampling methods, such as canisters and adsorption/thermal desorption (ATD) cartridges, along with gas chromatography (GC) analysis, have limitations related to their low time resolution, susceptibility to sampling artifacts, and limited range of measurable compounds (Hatch et al., 2018; Hatch et al., 2017). In addition to offline techniques, proton-transfer-reaction mass spectrometry (PTR-MS) has been widely used for the online measurement of volatile organic compounds (VOCs) in the atmosphere (Yuan et al., 2017). However, IVOCs still suffer from high losses in the sampling lines and PTR-MS drift tubes. Furthermore, most studies have focused on either primary or aged emissions, with very few examining the real-time influence of combustion conditions on the composition of emitted organic vapors (Bruns et al., 2016; Akherati et al., 2020; Tkacik et al., 2017). The recently developed Vocus proton-transfer-reaction time-of-flight (PTR-TOF) mass spectrometer (hereafter Vocus) has greatly enhanced sensitivity due to a newly designed chemical ionization source (Krechmer et al., 2018), and it can detect a broader spectrum of VOCs, IVOCs, and their oxygenated products (up to six to eight oxygen atoms for monoterpene oxidation products) (Li et al., 2020; Wang et al., 2021; Riva et al., 2019). With a novel design and chemical ionization source, the Vocus allows real-time characterization of gas-phase emissions during various burning phases (e.g., flaming and non-flaming phases) and identifies the potential markers for a wide range of fuels.

The present study compares real-time emissions from different combustion fuels. We begin by demonstrating that the evolution of gas-phase emissions during burning cycles highlights the changes in the composition of the emissions. Then, we systematically characterize the composition of organic vapors using Vocus from a variety of burning fuels from both residential stoves (beech logs, spruce/pine logs, and coal) and open combustion (spruce/pine branches and needles, straw, cow dung). We evaluate the potential markers and EFs for different fuels and explore the dependence of individual organic vapor emission intensity, variability, and chemical composition on solid fuel types and combustion

phases. We also discuss potential markers for the burning fuels examined in this study. The potential markers are identified as statistical outliers determined with a Mann–Whitney test, consistent with previous measurements (Zhang et al., 2023). The differences in EFs and profiles between different combustibles can be considerable, and these results illustrate the importance of considering these emission sources individually. Measurements capable of identifying and quantifying rarely measured and presently unidentified emissions of organic vapors, particularly chemically complex SVOCs and IVOCs, are vital for advancing the current understanding of the impact of solid fuel combustion on air quality and climate.

## 2 Materials and methods

### 2.1 Fuel and burning types

The experiments were conducted at the Paul Scherrer Institute (PSI) in Villigen, Switzerland. The burning facility is part of the PSI Atmospheric Chemistry Simulation (PACS) chambers. Real-time characterization of the primary gas- and particle-phase emissions was carried out during 28 test burns. Six solid fuels were studied (coal briquettes and biomass fuels, beech logs, spruce/pine logs, fresh spruce/pine branches and needles, dry straw, cow dung), with 3 to 6 replicate burns. Material in the beech, spruce, and pine fuels (e.g., logs and needles) was sourced from a local forestry company in Würenlingen, Switzerland. Cow dung cakes (a mixture of cow dung and straw) were collected from Goyla Dairy in Delhi, India. Coal briquettes were purchased in Gansu, China (Ni et al., 2021; Klein et al., 2018).

With those six different fuels, we categorized six burning types for this experiment: (1) beech logs stove, (2) spruce/pine logs stove, (3) spruce/pine branches and needles open, (4) dry straw open, (5) cow dung open, and (6) coal stove. We selected these six solid fuels and conducted emissions tests to simulate certain types of burning found in the atmosphere. In the list above, (1) beech logs stove and (2) spruce/pine logs stove are representative of residential wood burning, as they are burned separately in a stove, consistent with the materials used in two previous articles (Bertrand et al., 2017; Bhattu et al., 2019). To represent forest fires or wildfire and agricultural field combustion, a mixture of (3) fresh spruce/pine branches and needles and (4) straw was combusted in an open stainless-steel cylinder (65 cm in diameter and 35 cm in height). Traditional cooking and heating practices in regions like India are represented by (5) the open burning of cow dung cakes by using half-open stoves (Loebel Roson et al., 2021). Finally, traditional cooking and heating practices in rural regions of developing countries are represented by (6) coal stove burning in a portable cast iron stove purchased from the local market (Liu et al., 2017). Of course, these conditions do not fully or accurately represent the conditions found in actual fires, which consist

of a variety of burning species (e.g., trees, underbrush, peat soils), but represent laboratory burning conditions.

### 2.2 Experimental setup and instrumentation

The experimental design is shown in Fig. S1 in the Supplement. In summary, it is made up of a burner and a set of diluters with heated lines. The zero air was provided by a zero air generator (737-250 series, AADCO Instruments, Inc., USA) for cleaning and dilution (Heringa et al., 2011; Bruns et al., 2015). The zero air generator takes ambient air and scrubs particulates and volatile organic compounds from the air, leaving a mixture that is largely made up of N<sub>2</sub>, O<sub>2</sub>, and Ar at ambient concentrations. Other trace gases are scrubbed to lower than atmospheric concentrations, including CO<sub>2</sub> (< 80 ppb) and CH<sub>4</sub> (< 40 ppb). Before each burn, a continuous stream of zero air was passed through the gas lines overnight to avoid cross-contamination between burns and to ensure a low background of VOCs. Once a burn is initiated from the various combustibles, emissions are sampled from the chimney through a heated line (473 K). The emissions (both gas- and particle phases) are then diluted by two Dekati diluters (DI-1000, Dekati Ltd.), diluting the emissions by a factor of ~ 100 (473 K; DI-1000, Dekati Ltd.). Note that beech log combustion cycles consist of a first cycle, referred to as the “first load”, and subsequent cycles, referred to as “reloads”. The first load consisted of cold-start, flaming, smoldering, and burn-out phases, and the reloads comprised warm-start, flaming, smoldering, and burn-out phases. Organic vapor emissions of solid fuel combustion are released within 10–30 min after loading, according to the properties of the fuels. We define the time until the full ignition duration for burning encompasses 80 % of the entire process, starting from loading the fuels to burn-out.

Numerous instruments were connected after the second Dekati diluter for the characterization of both the particulate and the gaseous phases. A scanning mobility particle sizer (SMPS; CPC 3022, TSI, and custom-built DMA) provided particle number size distribution information and was calibrated by using polystyrene latex (PSL) particle size standards (Wiedensohler et al., 2018; Sarangi et al., 2017). The non-refractory particle composition was monitored by a high-resolution time-of-flight aerosol mass spectrometer (HR-TOF-AMS; Aerodyne Research Inc.). AMS data were processed using SeQUential Igor data RetRiEvaL (SQUIRREL) v. 1.63 (D. Sueper, University of Colorado, Boulder, CO, USA) and Peak Integration and Key Analysis (PIKA) v. 1.23 to obtain mass spectra of identified ions in the  $m/z$  range of 12 to 120. Organic carbon (OC) is derived from the ratio of organic mass (OM) to OC (OM/OC) determined with high-resolution AMS analysis (Canagaratna et al., 2015). In the AMS mass spectra, the fraction of  $m/z$  60 ( $f_{60}$ ) represents the ratio of levoglucosan-like species (Schneider et al., 2006; Alfara et al., 2007). AMS was calibrated for ionization efficiency (IE) by a mass-based

method using  $\text{NH}_4\text{NO}_3$  particles (Tong et al., 2021). Black carbon (BC) was measured with an aethalometer (Magee Scientific aethalometer model AE33) (Drinovec et al., 2015) with a time resolution of 1 min. The maintenance and calibration are given in the AE33 user manual version 1.57. An LI-7000  $\text{CO}_2$  analyzer (LI-COR) and APMA-370 CO analyzer (Horiba) provided continuous measurements of carbon dioxide ( $\text{CO}_2$ ) and carbon monoxide (CO), respectively. The concentrations of total hydrocarbons (THCs) and methane ( $\text{CH}_4$ ) were monitored using a flame ionization detector monitor (THC monitor Horiba APHA-370).

We deployed a Vocus to measure organic vapors with a wider range of volatilities. A detailed description of the Vocus is provided elsewhere (Huang et al., 2021; Krechmer et al., 2018). For this study, the Vocus was operated with  $\text{H}_3\text{O}^+$  as the reagent ion. The sample air was drawn in through a 1 m long polytetrafluoroethylene (PTFE) tube (6 mm o.d.) using a total sample flow of  $4.3 \text{ L min}^{-1}$ , which helped reduce the losses in the inlet wall and the sampling delay. Of the total sample flow, only  $100\text{--}150 \text{ cm}^3 \text{ min}^{-1}$  went to Vocus, and the rest was exhausted. The Vocus was calibrated before and after measurements every day using a multi-component standard cylinder (TOFWERK AG). Standard gases were diluted by the injection of zero air, producing mixing ratios of VOCs of around 20 ppbv. The calibration components were methanol, acetaldehyde, acetonitrile, acetone, acrylonitrile, isoprene, methyl ethyl ketone, benzene, toluene, *m*-xylene,  $\alpha$ -pinene, and 1,2,4-trimethylbenzene. The background measurements were performed using dry zero air every day. Data were recorded with a time resolution of 1 s. The raw data were processed using Tofware v3.2.3 software (TOFWERK and Aerodyne, Inc.). The standard non-targeted analysis workflow developed by TOFWERK was adopted for mass calibration and peak fitting. The mass transmission function and the ratios between the measured and calculated sensitivities for a series of ions were used to quantify the data and convert the ion counts to parts per billion by volume (ppbv). To calculate the mixing ratio for compounds not present in the calibration mixture, the slope of the linear fit was multiplied by the proton transfer rate constants ( $k_{\text{pr}}$ ), which are provided in Table S3 in the Supplement.

### 2.3 Data analysis

Modified combustion efficiency (MCE; Eq. 1) is an estimate of the relative amount of flaming and smoldering and is equal to

$$\text{MCE} = \frac{\Delta\text{CO}_2}{\Delta\text{CO} + \Delta\text{CO}_2}, \quad (1)$$

where  $\Delta\text{CO}$  and  $\Delta\text{CO}_2$  are the mixing ratios of CO and  $\text{CO}_2$  in excess of background (measured before the combustion), respectively (Christian et al., 2003). Generally, a higher MCE ( $> 0.9$ ) suggests dominantly flaming combus-

tion, whereas a lower MCE ( $< 0.9$ ) is mostly associated with smoldering combustion (Zhao et al., 2021; Zhang et al., 2022).

The emission factors (EFs;  $\text{g kg}^{-1}$ ) of species  $i$  was calculated, following a carbon mass balance approach (Andreae, 2019; Boubel et al., 1969; Nelson, 1982):

$$\text{EF}_i = \frac{m_i}{\Delta\text{mCO} + \Delta\text{mCO}_2 + \Delta\text{mCH}_4 + \Delta\text{mNMOGs} + \Delta\text{mOC} + \Delta\text{mBC}} \times W_C. \quad (2)$$

Here,  $m_i$  refers to the mass concentration of species  $i$ .  $\Delta\text{mCO}$ ,  $\Delta\text{mCO}_2$ ,  $\Delta\text{mCH}_4$ ,  $\Delta\text{mNMOGs}$ ,  $\Delta\text{mOC}$ , and  $\Delta\text{mBC}$  are the background-corrected carbon mass concentrations of carbon-containing species in the flue gas.  $W_C$  is the carbon mass fraction of the burning fuel. For the  $W_C$  in the fuel, a constant average value of 0.46 for wood (Bertrand et al., 2017), 0.45 for straw (Li et al., 2007), 0.45 for cow dung (Font-Palma, 2019), and 0.49 for coal (Zhang et al., 2000) was assumed. Changes in  $W_C$  over the burning cycle are expected to be small compared to the variability in pollutant emissions. The volatility (i.e., the saturation mass concentration,  $C^*$ ) for individual organic compounds was calculated based on the number of oxygen, carbon, and nitrogen atoms in the compound using the approach by Li et al. (2016):

$$\log_{10} C^* = \left( n_C^0 - n_C^i \right) b_C - n_O^i b_O - 2 \frac{n_C^i n_O^i}{n_C^i + n_O^i} b_{\text{CO}} - n_N^i b_N, \quad (3)$$

where  $n_C^0$  is the reference carbon number and  $n_C^i$ ,  $n_O^i$ , and  $n_N^i$  denote the numbers of carbon, oxygen, and nitrogen, respectively, in the compound.  $b_C$ ,  $b_O$ , and  $b_N$  are the contributions of each atom to  $\log_{10} C^*$ , respectively, and  $b_{\text{CO}}$  is the carbon–oxygen non-ideality. The parameters used in this analysis are presented in Table S1 in the Supplement. Most notably, the empirical approach used by Li et al. (2016) was derived with only a limited number of organonitrates, which could potentially introduce bias in estimating vapor pressure (Isaacman-Vanwertz and Aumont, 2021). To mitigate this bias, we modified the nitrogen coefficient for CHON formulas that can be forced to equal twice the negative of the oxygen atom ( $b_N = -2b_O$ ).

### 2.4 Identification of potential markers

In this study, the relative contribution of the mixing ratio for over 1500 species from six different fuels was quantified across all 28 test burns using the Vocus. To identify the potential markers of emissions from different fuels, we implemented the Mann–Whitney  $U$  test (Mann and Whitney, 1947; Wilcoxon, 1945) in MATLAB<sup>®</sup>. Mann–Whitney is a non-parametric test and has been applied in the selection of aerosol markers (Zhang et al., 2023), proteomic markers (White et al., 2019; Chen et al., 2012; Teunissen et al., 2011; Chmaj-Wierzchowska et al., 2015; Nomura et al., 2004), and

**Table 1.** Average EFs of CO, CO<sub>2</sub>, organic vapors, and PM and the MCE for six types of solid fuel.

Solid fuel type	Carbon content	MCE	Emission factors (g kg <sup>-1</sup> fuel)			
			CO	CO <sub>2</sub>	organic vapors	PM
Beech logs stove ( <i>n</i> = 6)	0.46	0.96 ± 0.03	38.9 ± 25.9	1409.4 ± 177.1	74.2 ± 42.9	2.5 ± 1.7
Spruce/pine logs stove ( <i>n</i> = 5)	0.46	0.97 ± 0.01	28.5 ± 14.3	1511.7 ± 68.5	44.9 ± 17.5	1 ± 0.6
Spruce/pine branches and needles open ( <i>n</i> = 3)	0.46	0.99 ± 0.001	2.8 ± 0.8	1579.2 ± 29.7	39.8 ± 11.4	0.9 ± 0.4
Straw open ( <i>n</i> = 4)	0.45	0.97 ± 0.01	24.4 ± 6.6	1488.4 ± 87.2	42.6 ± 33.7	2.8 ± 0.7
Cow dung open ( <i>n</i> = 5)	0.45	0.95 ± 0.03	53.9 ± 27.2	1541.8 ± 50.2	4.8 ± 0.98	1.2 ± 0.61
Coal stove ( <i>n</i> = 5)	0.49	0.96 ± 0.01	40.6 ± 12.6	1680.2 ± 32.7	11.5 ± 2.6	0.9 ± 0.3

other biomarkers (including measurements with a PTR-MS) (Jasperse et al., 2007; Nagai et al., 2020; Sun et al., 2019; Tritten et al., 2013). It is used for between-group comparisons when the dependent variable is ordinal or continuous and not assumed to follow a normal distribution with small sample sizes. This test takes two data samples as parameters, uses the ranks as a measure of central tendency, and then returns the test results with a *p* value to indicate the statistical significance. When the *p* value is lower than the significance level of 0.1 (a commonly used *p* value to study statistical significance in atmospheric research), the median of the tested sample is significantly high or low in the two-tailed test. The molecules from a specific class of fuel that satisfy the pairwise comparison test between one fuel, referred to as fuel *j*, and other types of fuel were determined to be significantly high- or low-fraction ions in fuel *j*. These ions have the potential to serve as potential markers for fuel *j*. In addition, the fold change (FC) of ion *i* in fuel *j* was calculated using Eq. (4),

$$FC_{i,j} = \frac{f_{i,j}}{f_{i,other}}, \quad (4)$$

where  $f_{i,j}$  represents the fraction of ion *i* in the mass spectra profiles of fuel *j* and  $f_{i,other}$  represents the average fraction of ion *i* in the mass spectra from the other fuels.

To identify potential markers, the Mann–Whitney *U* test was used to compare the emissions observed for one type of fuel (e.g., spruce/pine logs), with the gaseous emissions observed for other fuels. The data used for the comparison were the average composition measured throughout a full burning cycle, excluding the initial ignition period. However, due to the similarity in solid fuel types between burning spruce/pine logs and between spruce/pine branches and needles, they were categorized as separate solid fuel types for this test and not compared with each other but were only compared with the other four types of fuels. This could result in the loss of many same markers, since these two types of fuel actually come from the same type of tree. Therefore, when identifying markers for spruce/pine logs using the Mann–Whitney *U* test, spruce/pine branches and needles were not included in the comparison group. Similarly, due to the composition of cow dung “cakes”, which are a mixture of dried cow dung

and crop residues, the approach used in the Mann–Whitney *U* test is consistent with the above method.

### 3 Results and discussion

#### 3.1 The characteristics of EF and MCE from different solid fuel types

The average EFs of CO, CO<sub>2</sub>, organic vapors, and particular matter (PM) in g kg<sup>-1</sup> and the MCE values calculated for the six types of fuel are shown in Table 1. Detailed EFs and MCE values for each experiment can be found in Table S2 in the Supplement. The average MCE value depends on the solid fuel type and the combustion phase (flaming and smoldering) that is occurring. The lowest MCE values, 0.90, were observed during the smoldering phase of the stove-burning of beech logs, while the highest values (0.99) were recorded during the flaming phase of the spruce/pine branches and the open burning of needles. In all experiments, the highest EFs for a single gas-phase species correspond to CO<sub>2</sub> (1136.2–1711.7 g kg<sup>-1</sup>). Coal burning has the highest average CO EFs (40.6 ± 12.6 g kg<sup>-1</sup>) and CO<sub>2</sub> EFs (1680.2 ± 32.7 g kg<sup>-1</sup>).

Total organic vapor EFs reported in Table 1 refer to species quantified using the Vocus. The average EFs of organic vapors (in the range of 4.8 to 74.2 g kg<sup>-1</sup>) and the standard deviation are calculated based on the average EFs for the repeatable experiments, which depend on the combustion phases and solid fuel types. Generally, lower MCE values correspond to higher organic vapor EFs within a given class of burning fuel (Fig. S2a in the Supplement). For instance, smoldering beech logs resulted in significantly higher average organic vapor EFs (74.2 ± 42.9 g kg<sup>-1</sup>) compared to burning spruce/pine logs. Spruce/pine stove and open burning, dominated by the flaming phase (average MCE > 0.95), exhibited average organic vapor EFs of 44.9 ± 17.5 g kg<sup>-1</sup> and 39.8 ± 11.4 g kg<sup>-1</sup>, respectively. This value is higher than the previous study (37.3 g kg<sup>-1</sup>), even though the difference is in the uncertainty levels, which can be attributed to the more extensive analysis of organic vapor in our study (Hatch et al., 2017). Despite the slight difference in MCE for some experiments, the increasing EFs for organic vapors with at least six carbon atoms per molecule (≥ C6) as proxy

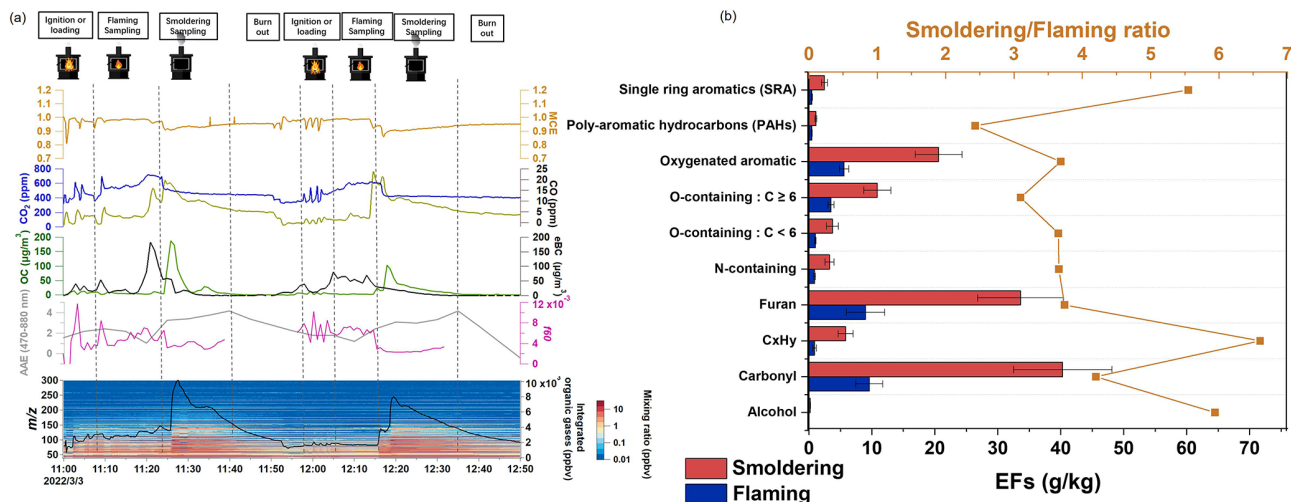


**Figure 1.** (a) Temporal profiles of mixing ratios measured by Vocus and the evolution of CO, CO<sub>2</sub>, AAE, *f*60, MCE, and key aerosol compositions during burning cycles of beech log stove burning. (b) Geometric mean of the primary EFs for gas-phase species of different functional groups during the flaming and smoldering phase (the flaming and smoldering were separated by the experimental record and calculated MCE). Error bars correspond to the sample geometric standard deviation of the replicates. The square represents the mixing ratio between smoldering and flaming. In this study, the MCE is used to indicate the flaming stage and smoldering, and a significant decrease in MAC and CO<sub>2</sub> was observed from the flaming phase to the smoldering phase.

SOA precursors were observed with lower MCE (Fig. S2b) (Bruns et al., 2016). Moreover, the EFs of these SOA precursors are much higher than the primary biomass burning organic aerosol (BBOA), which suggests a higher potential for SOA formation. Notably, the EFs of organic vapors from cow dung and coal were relatively low, at  $4.8 \pm 0.98$  and  $11.5 \pm 2.6 \text{ g kg}^{-1}$ , respectively. Our EFs align well with previously reported volatile organic compound EFs from bituminous coal combustion under similar conditions (range of 1.5 to  $14.1 \text{ g kg}^{-1}$ ) reported by Klein et al. (2018).

### 3.2 Comparison between flaming and smoldering of wood burning

Figure 1a shows a typical burning cycle during beech log wood experiments, with distinct emission characteristics between flaming and smoldering phases. In the top panel, the MCE, CO, and CO<sub>2</sub> concentrations, along with our experimental records, are used to indicate the flaming and smoldering stages. The flaming phase shows considerable BC emission, while the smoldering phase is dominated by organic aerosol emissions without visible flame. The absorption Ångström exponent (AAE) during the smoldering phase is approximately twice that of the flaming phase, possibly due to the presence of “brown carbon” in organic aerosols. *f*60 represents the prevalence of primary combustion products, such as levoglucosan, and is used as an indicator for fresh BB emissions (Schneider et al., 2006; Alfara et al., 2007). During the starting/flaming phase, when the temperature is higher, *f*60 increases, whereas, for lower temperatures in the smoldering phase, *f*60 decreases (Weimer et al.,

2008). The mixing ratio of most of the compounds correlates negatively with the MCE, as expected, with a significant increase in the smoldering phase (Fig. 1a and S3 in the Supplement). However, some compounds like benzene have different enhancement rates from flaming to smoldering, which is similar to previous studies (Warneke et al., 2011).

Figure 1b illustrates the measured EFs for flaming and smoldering wood fire stages. On average, EFs for organic vapors in the flaming stage are approximately 4 times lower ( $31.4 \pm 7.1 \text{ g kg}^{-1}$ ) than those in the smoldering fire stages ( $121.9 \pm 24 \text{ g kg}^{-1}$ ). Despite significant variability in the strength of organic vapor emissions (EFs), the average carbon and oxygen distribution of organic vapors remained largely consistent across the combustion phases (Fig. S4 in the Supplement). Hardwood (beech) is a fibrous substance primarily composed of three chemical elements (carbon, hydrogen, and oxygen), and these basic elements are incorporated into several organic compounds, i.e., cellulose, hemicellulose, lignin, and extractives formed into a cellular structure (Asif, 2009). The flaming stage is associated with more complete oxidation with a relatively higher contribution of oxygenated VOCs (OVOCs; e.g., furan, oxygenated aromatics, O-containing; Fig. S5 in the Supplement). Conversely, during the smoldering stage, more CO and organic vapors are emitted relative to the flaming stage (Fig. 1a). OVOCs, such as carbonyl, furan, oxygenated aromatics, and O-containing species, form the major fraction (> 88 %) of emissions in both flaming and smoldering fires. They are followed by the sum of C<sub>x</sub>H<sub>y</sub>, and SRA (5 %–10 %). As shown in Fig. S6 in the Supplement, the volatility distribution of the emissions between the flaming phase and the smoldering phase changes

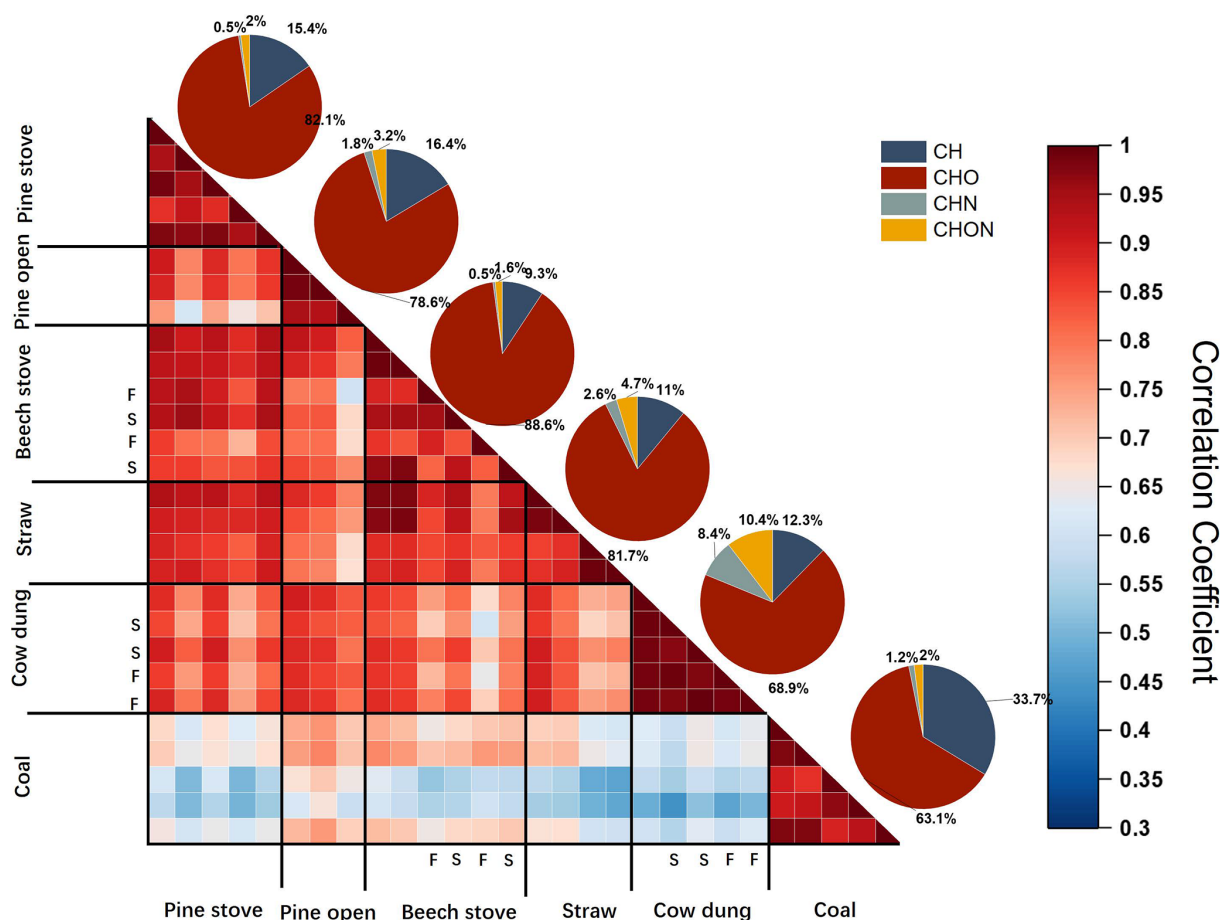


**Figure 2.** The correlation matrix of organic vapors measured with Vocus (F represents flaming phase, S represents smoldering phase, and unmarked columns and rows represent mixtures of both flaming and smoldering phases). Pie charts showing the contribution of elemental families are on the diagonal.

slightly with a decrease in the IVOCs from 25.8 % (flaming) to 20.2 % (smoldering). However, in absolute terms, all emissions are enhanced during the smoldering phase, including IVOCs, due to the increased EFs during the smoldering phase. As Fig. 1b shows, on a relative scale, there is a higher contribution of single-ring aromatics and  $C_xH_y$  in the smoldering phase than in the flaming phase. Within these measurements in our residential stove, we observe relatively small differences in the composition relative to the large increase in EFs when moving from flaming to smoldering conditions.

### 3.3 The characteristics of organic vapor from different solid fuel types

#### 3.3.1 Chemical composition of organic vapor from combustion

To assess the feasibility of distinguishing differences between combustion solid fuel types based on the measured species, we evaluated the similarity of the mass spectra ob-

tained from each experiment using the correlation coefficient ( $r$ ), as shown in Fig. 2; organic vapors from the same burning fuel are strongly correlated (0.82–0.99), indicating the general repeatability of the experiments. Furthermore, we observed a weak intra-fuel correlation between coal and other biomass sources (0.44–0.78), suggesting significant differences in chemical composition. By contrast, the separation between different solid fuel type is not stark, and all possess a correlation between 0.6–0.98. Overall, the correlation coefficient highlights similarities between all biomass-based emissions, which will now be discussed in detail.

Figure 2 also shows the average mixing ratio contribution of full ignition duration from  $m/z$  40 to 300 for each experiment and is categorized into  $C_xH_y$ ,  $C_xH_yO_z$ ,  $C_xH_yN$ , and  $C_xH_yO_zN$  families based on their elemental composition. In all organic vapors, the  $C_xH_yO_z$  family is the most abundant group, making the largest contribution to beech logs (88.6 %), spruce/pines logs (82.1 %), and straw (81.7 %). These percentages are higher than those for coal (63.1 %) and cow dung (68.9 %). Coal burning results in considerably

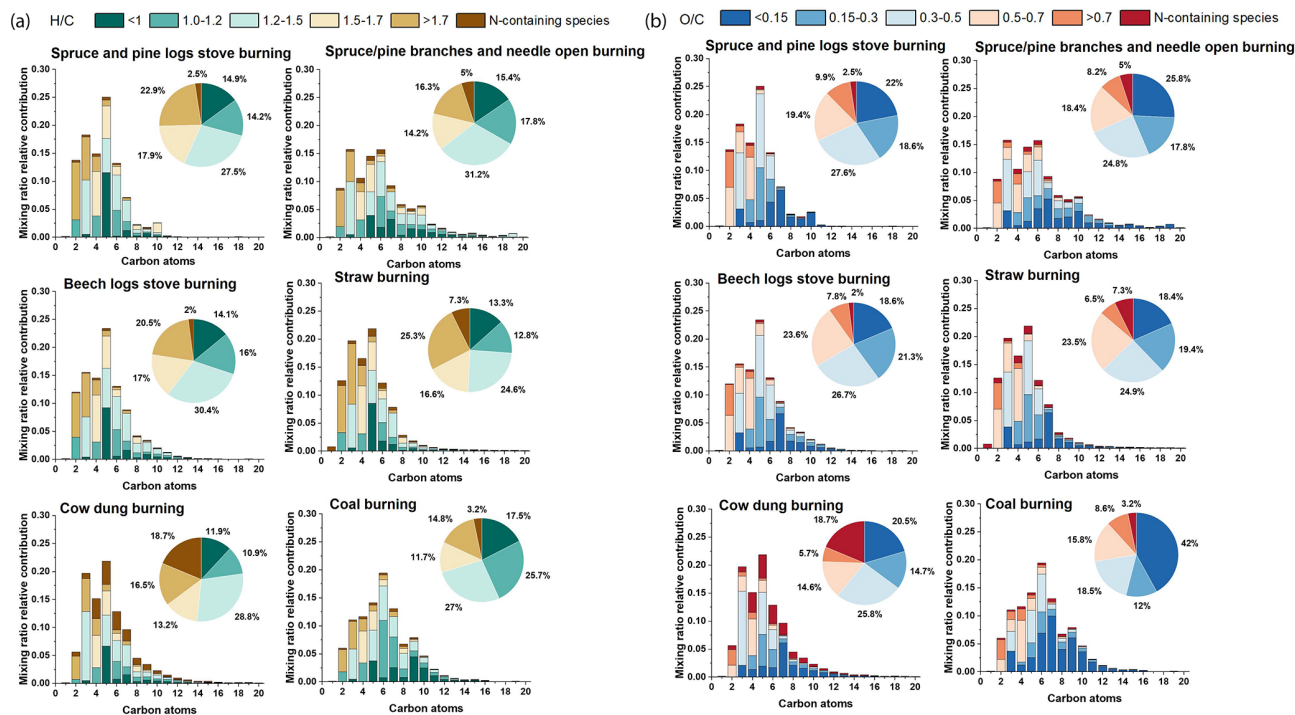


**Figure 3.** The average carbon distribution is colored by the H/C (a) and O/C (b) for non-N-containing species. The pie charts are the corresponding contribution of a range of H/C or O/C ratios.

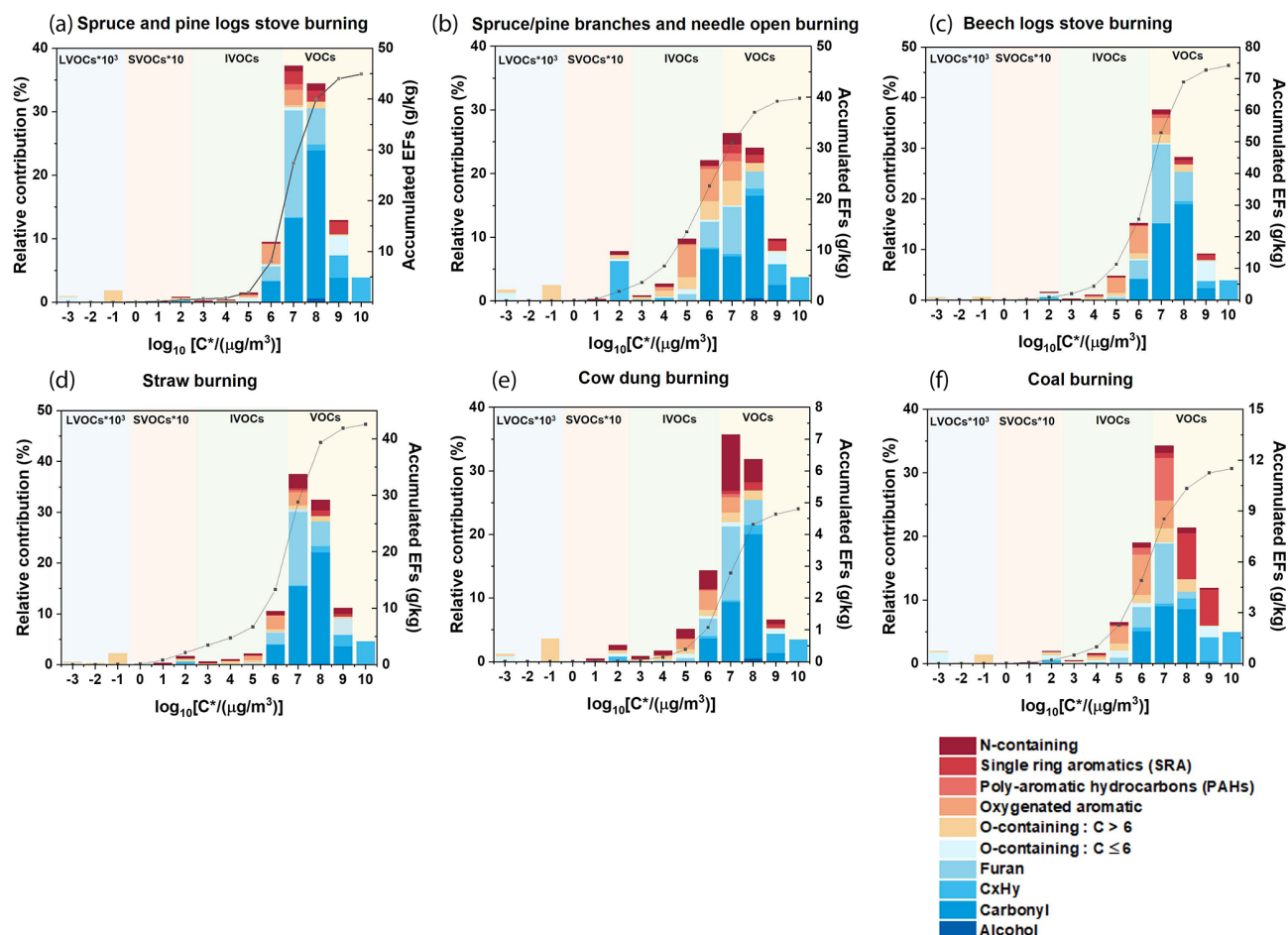
higher contributions in the  $C_xH_y$  families (33.7 %) than in beech logs (9.3 %), consistent with the bulk chemical composition of the fuels.

Figure 3 separates emitted compounds based on their carbon ( $x$ -axis) numbers. The dominant signals in organic vapors for all fuels are attributed to C3–6 compounds, while more species with higher carbon numbers ( $\#C > 10$ ) are observed in the open burning of spruce/pine branches and needles. The bin containing hydrogen-to-carbon ratios (H/C; calculated as the ratio of hydrogen atoms to carbon atoms in a molecule) between 1.2 and 1.5 has the largest contribution in all fuels except straw, ranging from 27 % to 31.2 %. Oxygen-to-carbon ratios (O/C; calculated as the ratio of oxygen atoms to carbon atoms in a molecule) less than 0.15 contribute significantly to coal burning (42 %), which corresponds to the high proportion of  $C_xH_y$  families (Fig. 2). Wood and straw burning emitted more oxygenated organic vapors than coal and cow dung burning with more contribution of higher O/C species (O/C > 0.5). The results show similarities to the comparison between burning wood and cow dung in the particle phase (Zhang et al., 2023). Specifically, cow dung exhibits a lower fraction of high O/C (0.22) compared to other fuels studied.

We categorized organic vapors by functional groups into 10 classes based on the classifications used in Bhattu et al. (2019). These classes include alcohols, carbonyls (including acid), hydrocarbons, furans, N-containing compounds, O-containing < 6 (where the number of carbon atoms is

less than 6), O-containing  $\geq 6$  (where the number of carbon atoms is equal to or greater than 6), oxygenated aromatics, polycyclic aromatic hydrocarbons (PAHs), and single-ring aromatics (SRA). Figures S7 and S8 in the Supplement show a comparison of the organic vapor composition observed from different solid fuel types. The measured emissions exhibit significantly different compositions, reflecting the variability in organic components produced from different solid fuel types. The emissions of all solid fuels are overwhelmingly dominated by carbonyls in the range of 23.1 % (coal) to 45.1 % (straw). For all emissions, furans represent the second largest group and account for more than 14 % of the emissions. Comparatively, aromatic compounds are less significant in BB: 5.9 %–12 % for oxygenated aromatics, 0.5 %–2.1 % for PAHs, and 2.1 %–5.8 % for SRA. In contrast, aromatic emissions are relatively larger in coal burning emissions (13.6 %, 8.1 %, and 13.8 %, respectively). Also, we note a specific difference in the oxygenated aromatic compounds and those with  $C > 6$  for open wood burning conditions, compared to the stove. This difference may be driven by the difference in the water content of the wood, which is significantly higher for open wood burning (30 %–40 %) compared to stove burning (10 %–12 %). The increase in these oxygenated components comes at the expense of species containing carbonyl and furan functionalities.

Generally, the total fraction of nitrogen-containing species ( $C_xH_yN$  and  $C_xH_yO_zN$ ) is significantly higher in the organic vapors emitted from open burning of cow dung (18.8 %)



**Figure 4.** Volatility and average accumulated EFs (assume the average molecular weight of each bin is same), with the distribution of primary emissions as a function of binned saturation vapor concentration. Shaded areas indicate the volatility ranges in units of  $\mu\text{g m}^{-3}$ : VOCs (yellow) as  $\log_{10}(C^*) > 6.5$ , IVOCs (blue) as  $\log_{10}(C^*)$  between 6.5 to 2.5, semi-VOCs (SVOCs; green) as  $\log_{10}(C^*)$  between 2.5 to  $-0.5$ , and low-VOCs (LVOCs; orange) as  $\log_{10}(C^*) < -0.5$ . The relative contributions of LVOCs and SVOCs are multiplied by a factor of 1000 and 10, respectively.

compared to the other fuels (2.1 % to 7.3 %). This trend is consistent with both our results from aerosol composition measurement and previous literature (Stewart et al., 2021b; Zhang et al., 2023; Loebel Roson et al., 2021). Generally, nitrogen-containing compounds in cow dung consist mainly of one nitrogen atom and have a wide range of carbon numbers between 2 and 7 (Fig. 3). Stewart et al. (2021a) also reported that cow dung was the largest emitter of nitrogen-containing organic vapors than other fuelwood and crops in India, releasing large amounts of acetonitrile and nitriles. These nitrogen-containing organic vapors are likely formed from the volatilization and decomposition of nitrogen-containing compounds within the cow dung cake, such as free amino acids, pyrroline, pyridine, and chlorophyll (Ren and Zhao, 2015; Burling et al., 2010).

### 3.3.2 Volatility of organic compounds

The parameterization described in Sect. 2.4 uses the modified approach of Li et al. (2016) to estimate the volatility of each of the measured compounds by the Vocus in  $\log_{10}(C^*)$  ( $\mu\text{g m}^{-3}$ ). The gaseous organic compounds were grouped into a 14-bin volatility basis set (VBS) (Donahue et al., 2006) (Fig. 4). Following the suggestions in recent papers (Wang et al., 2024; Li et al., 2023; Donahue et al., 2012; Huang et al., 2021; Schervish and Donahue, 2020), the volatility was aggregated into four main classes with units of micrograms per cubic meter ( $\mu\text{g m}^{-3}$ ): VOCs as  $\log_{10}(C^*) > 6.5$ , IVOCs as  $\log_{10}(C^*)$  between 6.5 to 2.5, semi-VOCs (SVOCs) as  $\log_{10}(C^*)$  between 2.5 to  $-0.5$ , and low-VOCs (LVOCs) as  $\log_{10}(C^*) < -0.5$ .

Comparison and compilation of organic vapors sorted by volatility and functional group classification are shown in Fig. 4, and the distribution of average EFs as a function of

binned saturation vapor concentration is shown. The VOC class was found to be the most abundant, ranging from 58.7 % to 87 % (Fig. S9 in the Supplement). For all burning types, carbonyls, furans, and SRA families are overwhelmingly dominant in VOCs, accounting for more than 60 % of the VOC emissions. The high fraction of oxygenated VOCs like carbonyls in BB emissions is in stark contrast to VOCs emitted from coal combustion, which is dominated by aromatic hydrocarbon emissions, particularly PAHs. This difference may be attributed to the condensed structure of coal and the lack of oxygen within the fuel itself. PAHs are a group of organic matter compounds containing multiple aromatic rings that mainly result from incomplete combustion (Masstral and Callen, 2000).

IVOCs also constituted a considerable fraction in solid-fuel combustions (from 12.6 % to 39.3 %), particularly in spruce/pine branches and needles (39.3 %), cow dung (24.3 %), and coal (31.1 %) (Fig. S9). Significant differences in the bulk volatility of organic compounds were observed among different types of wood burning. In general, the open burning of spruce/pine branches and needles released a higher proportion of IVOCs (39.3 %) into the gas phase compared to stove log burning (12.6 % and 23.9 %). This difference may be attributed to a lower percentage of terpenes in woody tissues compared to needle/leaf tissues (Greenberg et al., 2006). In addition, the open burning of wood has both a significantly larger water content and oxygen content than stove burning, which enhances the formation of partially oxidized organic compounds. Within the open-burning experiments, the oxygenated molecules (both aromatics and  $C \geq 6$ ) are enhanced relative to the other experiments and result in the largest EF of IVOCs. In addition to the burning conditions, the fuel properties are also an important factor affecting the IVOC component. Notably, cow dung comprised a higher fraction of N-containing species within their IVOC emissions compared to other fuels. The emissions of IVOCs characterized and quantified in this study are important for the estimation and modeling of aged emissions and their propensity to be able to form secondary organic aerosol.

### 3.4 Chemical characteristics of dominant compounds from all biomass fuels and identification of potential markers for specific solid fuels

#### 3.4.1 Chemical characteristics of dominant compounds from all biomass fuels

To conduct a comprehensive analysis aimed at identifying potential markers among emissions, the Mann–Whitney  $U$  test (refer to Sect. 2.4) was performed on the relative contribution of primary organic vapors derived from various fuels as measured by the Vocus. The results of the pairwise Mann–Whitney test are presented in Fig. S10 in the Supplement, illustrating the average  $-\log_{10} p$  value as a function of the  $\log_2$  fold change (FC). Species that yield  $p$  values lower

than 0.1 in the two-tailed test for all pairwise comparisons are deemed significantly more abundant or scarce in a particular solid fuel type compared to all other fuels. These species are indicated as colored circles in Fig. 5. In cases where species do not meet this criterion once or multiple times, they are represented as gray circles, even if their average  $p$  value falls below 0.1. A higher  $-\log_{10} (p \text{ value})$  signifies a reduced likelihood that the fractional medians of two species are equivalent. Simultaneously, a greater FC (as per Eq. 4) indicates an increased presence of the species' fractional contribution in the tested fuel in comparison to the average contribution across all other fuels. This suggests a higher degree of exclusivity for this species in the given context. The potential markers,  $p$  values, fold changes, and threshold results are listed in Table S3.

As shown in Fig. 2, biomass fuels (such as logs, branches, needles, straw, and cow dung) were analyzed separately from coal due to their distinct characteristics. To address this distinction, we characterized the dominant compounds across various biomass fuels by setting a threshold (relative mixing ratio contribution  $\geq 0.1$  %) for compounds that are not potential markers of one specific biomass fuel. This approach allowed us to identify compounds that are more readily detectable in complex environments. As shown in Fig. S11 in the Supplement, the gas-phase analysis revealed several dominant compounds,  $C_5H_4O_2$  (furfural; 2.2 %–10.1 %),  $C_2H_4O_2$  (acetic acid; 2.1 %–5.8 %),  $C_3H_6O_2$  (methyl acetate; 1.7 %–4.6 %), and  $C_2H_4O$  (acetaldehyde; 1.3 %–3.9 %), which were also reported in prior studies on BB (Bruns et al., 2017; Stockwell et al., 2015; Christian, 2004; Sarkar et al., 2016). Furthermore, the category of dominant compounds represents the primary set of compounds associated with BB, contributing 46 % to 69 % of the emissions (Fig. S12 in the Supplement). Carter et al. (2022) expand the representation of fire organic vapors in a global chemical transport model, GEOS-Chem, which contributes substantially to atmospheric reactivity, both locally and globally. Our results could provide more input information for global or regional chemistry transport models.

#### 3.4.2 Identification of potential markers for specific solid fuels

Mass defect plots of potential markers are visualized in Fig. 5 for each burning source. Many potential markers are identified for each unique type of burning (Table S3). As shown in Fig. 5, potential markers of all wood burning are mainly composed of compounds from the  $C_xH_y$  and  $C_xH_yO_z$  family. However, the potential markers for spruce/pine branches and needles have higher molecular weights and are more oxidized, which aligns with their characteristics of the mass spectrum. In contrast, compounds from the open burning of straw and cow dung contribute considerably more to nitrogen-containing families but less to oxygen-containing species, consistent with their bulk chemical composition

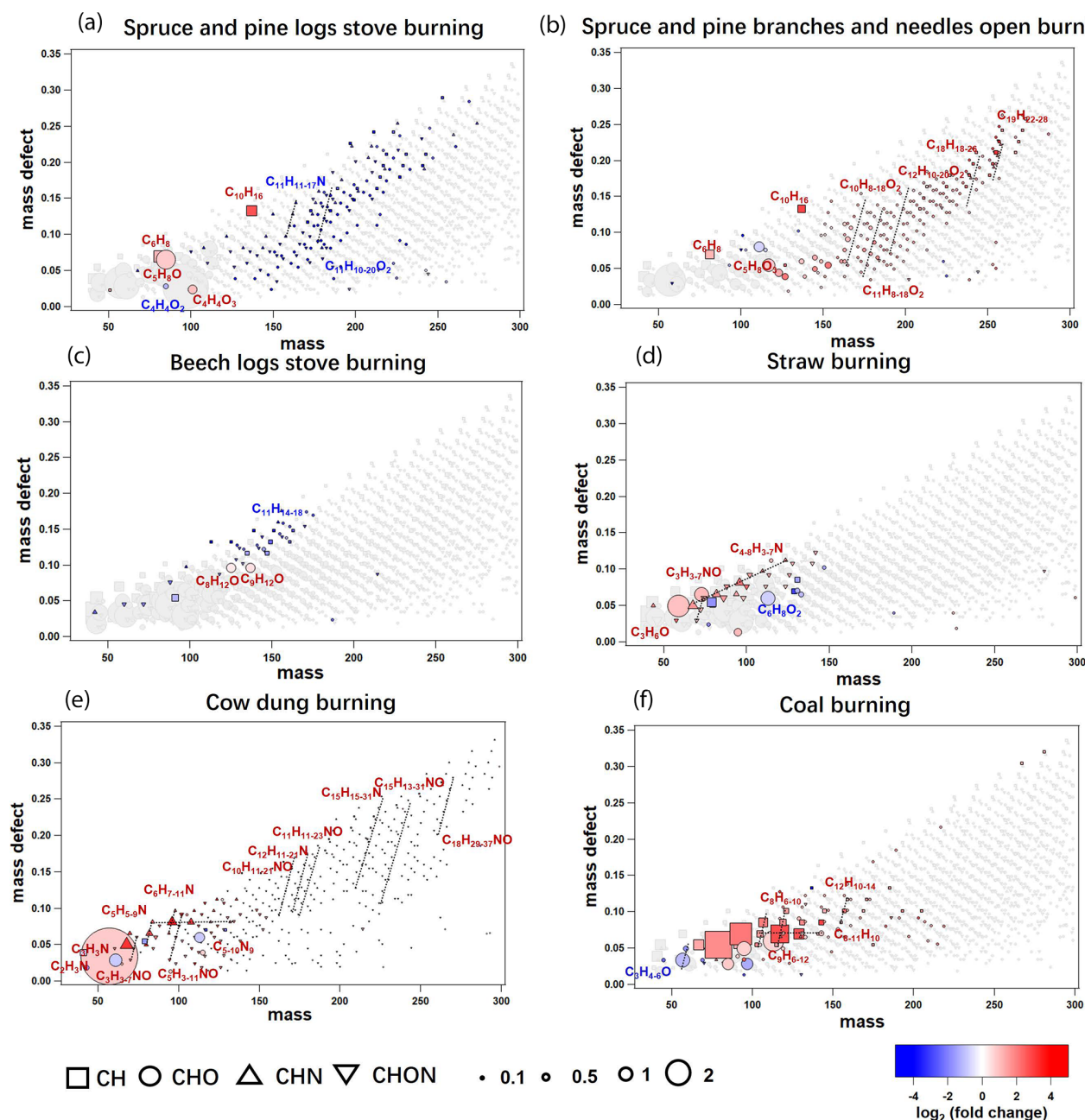


**Figure 5.** Mass defect plots identifying potential markers sized by the square root of fractional contribution (%) and colored by  $\log_2$  (the fold change). The dashed line represents the series of homologues.

characteristics. Additionally, potential markers for coal consist mainly of compounds from the  $C_xH_y$  family, which also aligns with its bulk chemical composition and relatively higher H/C ratios (Fig. 3).

For all softwood (i.e., spruce/pine logs and spruce/pine branches and needles in this study), monoterpenes ( $C_{10}H_{16}$ ) are a potential marker along with the fragment at  $m/z$  81.07 ( $C_6H_8$ ). However, monoterpenes cannot exclusively be related to BB given their abundance in the atmosphere.

Monoterpenes are also the biogenic volatile organic compounds (BVOCs) emitted from natural trees and other vegetation (Hellén et al., 2012). However, the emission rates of terpenes vary with season, with a higher rate in spring and summer and a lower rate in autumn and winter (He et al., 2000; Noe et al., 2012). In winter, monoterpenes could be a potential marker for softwood burning due to minor natural emissions from spruce, but, in summer, terpene emissions from natural trees would dominate the contribution,

making them a non-potential marker. P-cumenol ( $C_9H_{12}O$ ), as one of the potential markers for beech logs, was discovered to be one of the prominent products of beech wood pyrolysis of lignins (Sengpiel et al., 2019; Keller et al., 2020). Homologues of  $C_{10}H_{8-18}O_2$  are determined for spruce/pine branches and needles, with  $C_{10}H_{10}O_2$  being  $\beta$ -phenylacrylic acid, which is one of the main chemical compositions of the extract of the cedar pine needle.  $C_{10}H_{14}O_2$  could be 1-guaiacylpropane, which is proposed as a potential marker for coniferyl-type lignin pyrolysis products from pine (Simoneit et al., 1993; Liu et al., 2021). Homologues of  $C_{11}H_{8-18}O_2$  are also seen, for example,  $C_{11}H_{14}O_2$ , likely 1-(3,4-dimethoxyphenyl)-1-propene, which is stated as a representative compound found in lignin (Alves et al., 2003; Hill Bembenic, 2011).

Noticeably, cow dung has a significantly different chemical composition. As a result, many potential markers are identified from the burning of cow dung compared to other fuels. These potential markers predominantly contain nitrogen in chemical composition and overlap all potential markers for straw, owing to the mixture of dried cow dung and crop residues in “cow dung cakes”. Many nitrogen-containing potential markers are found in straw and cow dung, such as  $C_4H_5N$ ,  $C_5H_5N$ ,  $C_5H_7N$ , and  $C_6H_7N$ , which could likely be assigned to pyrrole, pyridine, methylpyrrole, and methyl pyridines, respectively. Pyrolysis of the constituents in the crop residue is a probable pathway for these compounds (Ma and Hays, 2008). Acetonitrile ( $C_2H_3N$ ), acrylonitrile ( $C_3H_3N$ ), propanenitrile ( $C_3H_5NO$ ), and 4-methylpentanenitrile ( $C_6H_{11}N$ ) were found to be potential markers for cow dung, with generally higher FC and higher relative contribution. Additionally, several series of nitrogen-containing homologues are found, such as  $C_{10}H_{11-21}NO$ ,  $C_{12}H_{11-21}N$ ,  $C_{11}H_{11-23}NO$ , and  $C_{15}H_{15-31}N$ . These nitrogen-containing gases have also been detected, especially in emissions from cow dung cakes in India compared to fuelwood, and are likely formed from the volatilization and decomposition of nitrogen-containing compounds within the cow dung cakes. These compounds originate primarily from free amino acids but can also arise from pyrroline, pyridine, and chlorophyll (Stewart et al., 2021a).

Coal is also a distinct solid fuel compared to other biomass fuels in this study, showing a relatively lower correlation coefficient (Fig. 2). Consequently, many series of  $C_xH_y$  family homologues are found. Compounds with 9–12 carbon atoms, as shown in Fig. 5 for coal burning, could be PAH-related, such as  $C_9H_8$  (1-indene),  $C_{10}H_8$  (naphthalene),  $C_{10}H_{10}$  (1-methylnaphthalene),  $C_{12}H_{10}$  (acenaphthene), and  $C_{12}H_{12}$  (2,6-dimethylnaphthalene). The EFs of the potential markers also show an increasing trend with the decrease in MCE (Fig. S13 in the Supplement), which suggests that EFs of the potential markers are dependent not only upon the type of fuel burned but also on the burning condition.

## 4 Conclusions

In this study, we investigated emissions of organic vapors using Vocus during typical solid fuel combustion, including burning of beech logs, spruce/pine logs, spruce/pine branches and needles, straw, and cow dung and coal briquettes. Average EFs of CO, CO<sub>2</sub>, organic vapors, and PM were calculated. This work provides a comprehensive laboratory-based analysis of the chemical composition of organic vapors emitted from the different combustibles and different combustion phases. We discuss the prominent net combustion emissions from BB and identify new potential markers using the Mann–Whitney *U* test.

The results indicate that wood burning has higher organic vapor EFs compared to other fuels. The emissions varied significantly, ranging from 4.8 to 74.2 g kg<sup>-1</sup>, depending on the combustion phases and solid fuel types. Despite the slight difference in modified combustion efficiency (MCE) for some experiments, the increasing EFs for organic vapors were observed with lower MCE. Moreover, the EFs of these SOA precursors are much higher than the primary biomass burning organic aerosol (BBOA), which suggests a higher potential for SOA formation. Distinct particulate/gas emissions at different combustion phases are observed for stove burning of beech logs: initial compositions of flaming or smoldering plumes were dominated by BC or OA, respectively, with much higher organic vapor emission in smoldering. The relative contribution of different classes showed large similarities between the combustion phases in beech log stove burning, relative to the large change in EFs observed. Therefore, the enhanced EFs under smoldering conditions means there is a greater potential for SOA formation when compared to flaming conditions.

The  $C_xH_yO_z$  family is the most abundant group (63.1 % to 88.6 %) for all solid fuels, followed by  $C_xH_y$  (9.3 % to 33.7 %). A larger contribution of nitrogen-containing species ( $C_xH_yN$  and  $C_xH_yO_zN$ ) is found in cow dung burning, while coal burning has a higher contribution from the  $C_xH_y$  family. Moreover, the VOC class was found to be the most abundant (58.7 % to 87 %), followed by the IVOC class (12.6 % to 39.3 %). Primary semi-volatile/intermediate-volatility organic compounds (S/IVOCs) have been proposed as important SOA precursors from BB. Li et al. (2024) found that IVOCs from residential wood burning (~ 13 % of total organic vapors) can contribute ~ 70 % of the formed SOA. Overall, these data will help update the IVOC emission inventory and improve the estimates of SOA production. Specifically, these results demonstrate that open burning (e.g., wildfire) emissions have enhanced IVOC EFs, suggesting that the SOA potential from open-burning sources is larger in comparison to their wood stove counterparts.

However, each source generally emits a wide spectrum of organic vapor species, leading to considerable overlap between organic vapor species from different sources. Based on the Mann–Whitney *U*, we selected species that were

unique in certain emissions as possible potential markers for specific solid fuels and the dominant compounds for all biomass fuels. Due to minor natural emissions from spruce in summer, monoterpenes ( $C_{10}H_{16}$ ) and their fragments could be potential markers for all softwoods (i.e., pine logs and spruce/pine branches and needles in this study) in winter. More products of the pyrolysis of coniferyl-type lignin and the cedar pine needle extract could be found in spruce/pine branches and the open burning of needles (e.g.,  $C_{10}H_{14}O_2$ ,  $C_{11}H_{14}O_2$ ,  $C_{10}H_{10}O_2$ ). The prominent product ( $C_9H_{12}O$ ) resulting from the pyrolysis of beech lignin is identified as a potential marker for beech log stove burning. Many series of nitrogen-containing homologues and nitrogen-containing species (e.g., acetonitrile, acrylonitrile, propanenitrile, methylpentanenitrile) are identified (e.g.,  $C_{10}H_{11-21}NO$ ,  $C_{12}H_{11-21}N$ ,  $C_{11}H_{11-23}NO$ , and  $C_{15}H_{15-31}N$ ), particularly from the open burning of cow dung. Coal is a unique solid fuel compared to biomass, and more PAH-related potential markers are identified from coal burning with 9–12 carbons. These potential markers provide important support for future global or regional chemistry transport modeling and source apportionment. Overall, our study provides a comprehensive understanding of the molecular composition and volatility of primary organic compounds and new insights into the identification of potential markers from the burning of solid fuels.

**Data availability.** The data presented in the text and figures are available in the Zenodo online repository (<https://doi.org/10.5281/zenodo.14204572>).

**Supplement.** The supplement related to this article is available online at <https://doi.org/10.5194/acp-25-2707-2025-supplement>.

**Author contributions.** TW, JZ, HL, KL, KYC, EG, LK, DMB, and RLM conducted the burning experiments. TW analyzed the data and wrote the paper. MB, ZCJD, LK, DMB, KL, RLM, IEH, HL, JGS, and ASHP participated in the interpretation of data.

**Competing interests.** The contact author has declared that none of the authors has any competing interests.

**Disclaimer.** Publisher's note: Copernicus Publications remains neutral with regard to jurisdictional claims made in the text, published maps, institutional affiliations, or any other geographical representation in this paper. While Copernicus Publications makes every effort to include appropriate place names, the final responsibility lies with the authors.

**Acknowledgements.** This work was supported by the Swiss National Science Foundation (SNSF) SNF grant MOLORG (grant no. 200020\_188624), an SNSF Joint Research Project (grant no. IZLCZO\_189883), the PSI career return fellowship, and the European Union's Horizon 2020 research and innovation program under Marie Skłodowska-Curie grant no. 884104 (PSI-FELLOW-III-3i) and ATMO-ACCESS. PSI's atmospheric simulation chamber is a facility of ACTRIS ERIC and receives funding from the Swiss State Secretariat for Education, Research and Innovation (SERI grant).

**Financial support.** This work was supported by the Swiss National Science Foundation (SNSF) SNF grant MOLORG (grant no. 200020\_188624), an SNSF Joint Research Project (grant no. IZLCZO\_189883), the PSI career return fellowship, and the European Union's Horizon 2020 research and innovation program under the Marie Skłodowska-Curie grant no. 884104 (PSI-FELLOW-III-3i) and ATMO-ACCESS. PSI's atmospheric simulation chamber is a facility of ACTRIS ERIC and receives funding from the Swiss State Secretariat for Education, Research and Innovation (SERI grant).

**Review statement.** This paper was edited by Ivan Kourtchev and reviewed by David Weise and two anonymous referees.

## References

- Akagi, S. K., Yokelson, R. J., Wiedinmyer, C., Alvarado, M. J., Reid, J. S., Karl, T., Crounse, J. D., and Wennberg, P. O.: Emission factors for open and domestic biomass burning for use in atmospheric models, *Atmos. Chem. Phys.*, 11, 4039–4072, <https://doi.org/10.5194/acp-11-4039-2011>, 2011.
- Akherati, A., He, Y., Coggon, M. M., Koss, A. R., Hodshire, A. L., Sekimoto, K., Warneke, C., de Gouw, J., Yee, L., Seinfeld, J. H., Onasch, T. B., Herndon, S. C., Knighton, W. B., Cappa, C. D., Kleeman, M. J., Lim, C. Y., Kroll, J. H., Pierce, J. R., and Jathar, S. H.: Oxygenated Aromatic Compounds are Important Precursors of Secondary Organic Aerosol in Biomass-Burning Emissions, *Environ. Sci. Technol.*, 54, 8568–8579, <https://doi.org/10.1021/acs.est.0c01345>, 2020.
- Alfarra, M. R., Prevot, A. S., Szidat, S., Sandradewi, J., Weimer, S., Lanz, V. A., Schreiber, D., Mohr, M., and Baltensperger, U.: Identification of the mass spectral signature of organic aerosols from wood burning emissions, *Environ. Sci. Technol.*, 41, 5770–5777, 2007.
- Alves, V., Capanema, E., Chen, C.-L., and Gratzl, J.: Comparative studies on oxidation of lignin model compounds with hydrogen peroxide using Mn(IV)-Me3TACN and Mn(IV)-Me4DTNE as catalyst, *J. Mol. Catal. A-Chem.*, 206, 37–51, 2003.
- Andreae, M. O.: Emission of trace gases and aerosols from biomass burning – an updated assessment, *Atmos. Chem. Phys.*, 19, 8523–8546, <https://doi.org/10.5194/acp-19-8523-2019>, 2019.
- Asif, M.: Sustainability of timber, wood and bamboo in construction, in: Sustainability of construction materials, Woodhead Publishing, Elsevier, 31–54, <https://doi.org/10.1533/9781845695842.31>, 2009.

- Bailey, J., Gerasopoulos, E., Rojas-Rueda, D., and Benmarhnia, T.: Potential health and equity co-benefits related to the mitigation policies reducing air pollution from residential wood burning in Athens, Greece, *J. Environ. Sci. Heal. A*, 54, 1144–1151, 2019.
- Balakrishnan, K., Ramaswamy, P., Sambandam, S., Thangavel, G., Ghosh, S., Johnson, P., Mukhopadhyay, K., Venugopal, V., and Thanasekaraan, V.: Air pollution from household solid fuel combustion in India: an overview of exposure and health related information to inform health research priorities, *Global Health action*, 4, 5638, <https://doi.org/10.3402/gha.v4i0.5638>, 2011.
- Bertrand, A., Stefanelli, G., Bruns, E. A., Pieber, S. M., Temime-Roussel, B., Slowik, J. G., Prévôt, A. S. H., Wortham, H., El Haddad, I., and Marchand, N.: Primary emissions and secondary aerosol production potential from woodstoves for residential heating: Influence of the stove technology and combustion efficiency, *Atmos. Environ.*, 169, 65–79, <https://doi.org/10.1016/j.atmosenv.2017.09.005>, 2017.
- Bhattu, D., Zotter, P., Zhou, J., Stefanelli, G., Klein, F., Bertrand, A., Temime-Roussel, B., Marchand, N., Slowik, J. G., Baltensperger, U., Prevot, A. S. H., Nussbaumer, T., El Haddad, I., and Dommen, J.: Effect of Stove Technology and Combustion Conditions on Gas and Particulate Emissions from Residential Biomass Combustion, *Environ. Sci. Technol.*, 53, 2209–2219, <https://doi.org/10.1021/acs.est.8b05020>, 2019.
- Boubel, R. W., Darley, E. F., and Schuck, E. A.: Emissions from burning grass stubble and straw, *JAPCA J. Air Waste Ma.*, 19, 497–500, 1969.
- Bruns, E. A., El Haddad, I., Keller, A., Klein, F., Kumar, N. K., Pieber, S. M., Corbin, J. C., Slowik, J. G., Brune, W. H., Baltensperger, U., and Prévôt, A. S. H.: Inter-comparison of laboratory smog chamber and flow reactor systems on organic aerosol yield and composition, *Atmos. Meas. Tech.*, 8, 2315–2332, <https://doi.org/10.5194/amt-8-2315-2015>, 2015.
- Bruns, E. A., El Haddad, I., Slowik, J. G., Kilic, D., Klein, F., Baltensperger, U., and Prevot, A. S.: Identification of significant precursor gases of secondary organic aerosols from residential wood combustion, *Sci. Rep.*, 6, 27881, <https://doi.org/10.1038/srep27881>, 2016.
- Bruns, E. A., Slowik, J. G., El Haddad, I., Kilic, D., Klein, F., Dommen, J., Temime-Roussel, B., Marchand, N., Baltensperger, U., and Prévôt, A. S. H.: Characterization of gas-phase organics using proton transfer reaction time-of-flight mass spectrometry: fresh and aged residential wood combustion emissions, *Atmos. Chem. Phys.*, 17, 705–720, <https://doi.org/10.5194/acp-17-705-2017>, 2017.
- Burling, I. R., Yokelson, R. J., Griffith, D. W. T., Johnson, T. J., Veres, P., Roberts, J. M., Warneke, C., Urbanski, S. P., Reardon, J., Weise, D. R., Hao, W. M., and de Gouw, J.: Laboratory measurements of trace gas emissions from biomass burning of fuel types from the southeastern and southwestern United States, *Atmos. Chem. Phys.*, 10, 11115–11130, <https://doi.org/10.5194/acp-10-11115-2010>, 2010.
- Canagaratna, M. R., Jimenez, J. L., Kroll, J. H., Chen, Q., Kessler, S. H., Massoli, P., Hildebrandt Ruiz, L., Fortner, E., Williams, L. R., Wilson, K. R., Surratt, J. D., Donahue, N. M., Jayne, J. T., and Worsnop, D. R.: Elemental ratio measurements of organic compounds using aerosol mass spectrometry: characterization, improved calibration, and implications, *Atmos. Chem. Phys.*, 15, 253–272, <https://doi.org/10.5194/acp-15-253-2015>, 2015.
- Carter, T. S., Heald, C. L., Kroll, J. H., Apel, E. C., Blake, D., Coggon, M., Edtbauer, A., Gkatzelis, G., Hornbrook, R. S., Peischl, J., Pfannerstill, E. Y., Piel, F., Reijrink, N. G., Ringsdorf, A., Warneke, C., Williams, J., Wisthaler, A., and Xu, L.: An improved representation of fire non-methane organic gases (NMOGs) in models: emissions to reactivity, *Atmos. Chem. Phys.*, 22, 12093–12111, <https://doi.org/10.5194/acp-22-12093-2022>, 2022.
- Chandramouli, C. and General, R.: Census of india 2011, Provisional Population Totals, Government of India, New Delhi, 409–413, 2011.
- Chen, Y.-T., Chen, H.-W., Domanski, D., Smith, D. S., Liang, K.-H., Wu, C.-C., Chen, C.-L., Chung, T., Chen, M.-C., and Chang, Y.-S.: Multiplexed quantification of 63 proteins in human urine by multiple reaction monitoring-based mass spectrometry for discovery of potential bladder cancer biomarkers, *J. Proteomics*, 75, 3529–3545, 2012.
- Chmaj-Wierzchowska, K., Kampioni, M., Wilczak, M., Sajdak, S., and Opala, T.: Novel markers in the diagnostics of endometriomas: Urocortin, ghrelin, and leptin or leukocytes, fibrinogen, and CA-125?, *Taiwan J. Obstet. Gynec.*, 54, 126–130, 2015.
- Christian, T. J.: Comprehensive laboratory measurements of biomass-burning emissions: 2. First intercomparison of open-path FTIR, PTR-MS, and GC-MS/FID/ECD, *J. Geophys. Res.*, 109, <https://doi.org/10.1029/2003jd003874>, 2004.
- Christian, T. J., Kleiss, B., Yokelson, R. J., Holzinger, R., Crutzen, P., Hao, W. M., Saharjo, B., and Ward, D. E.: Comprehensive laboratory measurements of biomass-burning emissions: 1. Emissions from Indonesian, African, and other fuels, *J. Geophys. Res.-Atmos.*, 108, <https://doi.org/10.1029/2003JD003704>, 2003.
- Donahue, N. M., Robinson, A., Stanier, C., and Pandis, S.: Coupled partitioning, dilution, and chemical aging of semivolatile organics, *Environ. Sci. Technol.*, 40, 2635–2643, 2006.
- Donahue, N. M., Kroll, J. H., Pandis, S. N., and Robinson, A. L.: A two-dimensional volatility basis set – Part 2: Diagnostics of organic-aerosol evolution, *Atmos. Chem. Phys.*, 12, 615–634, <https://doi.org/10.5194/acp-12-615-2012>, 2012.
- Drinovec, L., Močnik, G., Zotter, P., Prévôt, A. S. H., Ruckstuhl, C., Coz, E., Rupakheti, M., Sciare, J., Müller, T., Wiedensohler, A., and Hansen, A. D. A.: The “dual-spot” Aethalometer: an improved measurement of aerosol black carbon with real-time loading compensation, *Atmos. Meas. Tech.*, 8, 1965–1979, <https://doi.org/10.5194/amt-8-1965-2015>, 2015.
- Font-Palma, C.: Methods for the Treatment of Cattle Manure – A Review, *C-Journal of Carbon Research*, 5, 27, <https://doi.org/10.3390/c5020027>, 2019.
- Font, A., Ciupek, K., Butterfield, D., and Fuller, G.: Long-term trends in particulate matter from wood burning in the United Kingdom: Dependence on weather and social factors, *Environ. Pollut.*, 314, 120105, <https://doi.org/10.1016/j.envpol.2022.120105>, 2022.
- Fourtziou, L., Liakakou, E., Stavroulas, I., Theodosi, C., Zarnas, P., Psiloglou, B., Sciare, J., Maggos, T., Bairachtari, K., and Bougiatioti, A.: Multi-tracer approach to characterize domestic wood burning in Athens (Greece) during wintertime, *Atmos. Environ.*, 148, 89–101, 2017.
- Greenberg, J. P., Friedli, H., Guenther, A. B., Hanson, D., Harley, P., and Karl, T.: Volatile organic emissions from the distilla-

- tion and pyrolysis of vegetation, *Atmos. Chem. Phys.*, 6, 81–91, <https://doi.org/10.5194/acp-6-81-2006>, 2006.
- Grieshop, A. P., Logue, J. M., Donahue, N. M., and Robinson, A. L.: Laboratory investigation of photochemical oxidation of organic aerosol from wood fires 1: measurement and simulation of organic aerosol evolution, *Atmos. Chem. Phys.*, 9, 1263–1277, <https://doi.org/10.5194/acp-9-1263-2009>, 2009.
- Guo, J., Wu, H., Zhao, Z., Wang, J., and Liao, H.: Review on health impacts from domestic coal burning: emphasis on endemic fluorosis in Guizhou Province, Southwest China, *Rev. Environ. Contam. T.*, 258, 1–25, 2021.
- Hatch, L. E., Yokelson, R. J., Stockwell, C. E., Veres, P. R., Simpson, I. J., Blake, D. R., Orlando, J. J., and Barsanti, K. C.: Multi-instrument comparison and compilation of non-methane organic gas emissions from biomass burning and implications for smoke-derived secondary organic aerosol precursors, *Atmos. Chem. Phys.*, 17, 1471–1489, <https://doi.org/10.5194/acp-17-1471-2017>, 2017.
- Hatch, L. E., Rivas-Ubach, A., Jen, C. N., Lipton, M., Goldstein, A. H., and Barsanti, K. C.: Measurements of I/SVOCs in biomass-burning smoke using solid-phase extraction disks and two-dimensional gas chromatography, *Atmos. Chem. Phys.*, 18, 17801–17817, <https://doi.org/10.5194/acp-18-17801-2018>, 2018.
- Hatch, L. E., Jen, C. N., Kreisberg, N. M., Selimovic, V., Yokelson, R. J., Stamatidis, C., York, R. A., Foster, D., Stephens, S. L., and Goldstein, A. H.: Highly speciated measurements of terpenoids emitted from laboratory and mixed-conifer forest prescribed fires, *Environ. Sci. Technol.*, 53, 9418–9428, 2019.
- He, C., Murray, F., and Lyons, T.: Seasonal variations in monoterpene emissions from Eucalyptus species, *Chemosphere*, 2, 65–76, 2000.
- Hellén, H., Tykkä, T., and Hakola, H.: Importance of monoterpenes and isoprene in urban air in northern Europe, *Atmos. Environ.*, 59, 59–66, <https://doi.org/10.1016/j.atmosenv.2012.04.049>, 2012.
- Heringa, M. F., DeCarlo, P. F., Chirico, R., Tritscher, T., Dommen, J., Weingartner, E., Richter, R., Wehrle, G., Prévôt, A. S. H., and Baltensperger, U.: Investigations of primary and secondary particulate matter of different wood combustion appliances with a high-resolution time-of-flight aerosol mass spectrometer, *Atmos. Chem. Phys.*, 11, 5945–5957, <https://doi.org/10.5194/acp-11-5945-2011>, 2011.
- Hill Bembenc, M. A.: The chemistry of subcritical water reactions of a hardwood derived lignin and lignin model compounds with nitrogen, hydrogen, carbon monoxide and carbon dioxide, Ph.D. dissertation, The Pennsylvania State University, University Park, PA, 2011.
- Hodzic, A., Jimenez, J. L., Madronich, S., Canagaratna, M. R., DeCarlo, P. F., Kleinman, L., and Fast, J.: Modeling organic aerosols in a megacity: potential contribution of semi-volatile and intermediate volatility primary organic compounds to secondary organic aerosol formation, *Atmos. Chem. Phys.*, 10, 5491–5514, <https://doi.org/10.5194/acp-10-5491-2010>, 2010.
- Huang, W., Li, H., Sarnela, N., Heikkinen, L., Tham, Y. J., Mikkilä, J., Thomas, S. J., Donahue, N. M., Kulmala, M., and Bianchi, F.: Measurement report: Molecular composition and volatility of gaseous organic compounds in a boreal forest – from volatile organic compounds to highly oxygenated organic molecules, *Atmos. Chem. Phys.*, 21, 8961–8977, <https://doi.org/10.5194/acp-21-8961-2021>, 2021.
- Isaacman-VanWertz, G. and Aumont, B.: Impact of organic molecular structure on the estimation of atmospherically relevant physicochemical parameters, *Atmos. Chem. Phys.*, 21, 6541–6563, <https://doi.org/10.5194/acp-21-6541-2021>, 2021.
- Jasperse, B., Jakobs, C., Eikelenboom, M. J., Dijkstra, C. D., Uitdehaag, B. M., Barkhof, F., Polman, C. H., and Teunissen, C. E.: N-acetylaspartic acid in cerebrospinal fluid of multiple sclerosis patients determined by gas-chromatography-mass spectrometry, *J. Neurol.*, 254, 631–637, 2007.
- Jin, L., Permar, W., Selimovic, V., Ketcherside, D., Yokelson, R. J., Hornbrook, R. S., Apel, E. C., Ku, I.-T., Collett Jr., J. L., Sullivan, A. P., Jaffe, D. A., Pierce, J. R., Fried, A., Coggon, M. M., Gkatzelis, G. I., Warneke, C., Fischer, E. V., and Hu, L.: Constraining emissions of volatile organic compounds from western US wildfires with WE-CAN and FIREX-AQ airborne observations, *Atmos. Chem. Phys.*, 23, 5969–5991, <https://doi.org/10.5194/acp-23-5969-2023>, 2023.
- Kalogridis, A.-C., Vratolis, S., Liakakou, E., Gerasopoulos, E., Mihalopoulos, N., and Eleftheriadis, K.: Assessment of wood burning versus fossil fuel contribution to wintertime black carbon and carbon monoxide concentrations in Athens, Greece, *Atmos. Chem. Phys.*, 18, 10219–10236, <https://doi.org/10.5194/acp-18-10219-2018>, 2018.
- Keller, R. G., Di Marino, D., Blindert, M., and Wessling, M.: Hydrotropic solutions enable homogeneous fenton treatment of lignin, *Ind. Eng. Chem. Res.*, 59, 4229–4238, 2020.
- Klein, F., Pieber, S. M., Ni, H., Stefanelli, G., Bertrand, A., Kilic, D., Pospisilova, V., Temime-Roussel, B., Marchand, N., El Haddad, I., Slowik, J. G., Baltensperger, U., Cao, J., Huang, R. J., and Prevot, A. S. H.: Characterization of Gas-Phase Organics Using Proton Transfer Reaction Time-of-Flight Mass Spectrometry: Residential Coal Combustion, *Environ. Sci. Technol.*, 52, 2612–2617, <https://doi.org/10.1021/acs.est.7b03960>, 2018.
- Koss, A. R., Sekimoto, K., Gilman, J. B., Selimovic, V., Coggon, M. M., Zarzana, K. J., Yuan, B., Lerner, B. M., Brown, S. S., Jimenez, J. L., Krechmer, J., Roberts, J. M., Warneke, C., Yokelson, R. J., and de Gouw, J.: Non-methane organic gas emissions from biomass burning: identification, quantification, and emission factors from PTR-ToF during the FIREX 2016 laboratory experiment, *Atmos. Chem. Phys.*, 18, 3299–3319, <https://doi.org/10.5194/acp-18-3299-2018>, 2018.
- Krechmer, J., Lopez-Hilfiker, F., Koss, A., Hutterli, M., Stoermer, C., Deming, B., Kimmel, J., Warneke, C., Holzinger, R., Jayne, J., Worsnop, D., Fuhrer, K., Gonin, M., and de Gouw, J.: Evaluation of a New Reagent-Ion Source and Focusing Ion-Molecule Reactor for Use in Proton-Transfer-Reaction Mass Spectrometry, *Anal. Chem.*, 90, 12011–12018, <https://doi.org/10.1021/acs.analchem.8b02641>, 2018.
- Kumar, V., Slowik, J. G., Baltensperger, U., Prevot, A. S. H., and Bell, D. M.: Time-Resolved Molecular Characterization of Secondary Organic Aerosol Formed from OH and NO(3) Radical Initiated Oxidation of a Mixture of Aromatic Precursors, *Environ. Sci. Technol.*, 57, 11572–11582, <https://doi.org/10.1021/acs.est.3c00225>, 2023.
- Li, H., Riva, M., Rantala, P., Heikkinen, L., Daellenbach, K., Krechmer, J. E., Flaud, P.-M., Worsnop, D., Kulmala, M., Villenave, E., Perraudin, E., Ehn, M., and Bianchi, F.: Terpenes and their ox-

- dation products in the French Landes forest: insights from Vocus PTR-TOF measurements, *Atmos. Chem. Phys.*, 20, 1941–1959, <https://doi.org/10.5194/acp-20-1941-2020>, 2020.
- Li, K., Zhang, J., Bell, D. M., Wang, T., Lamkaddam, H., Cui, T., Qi, L., Surdu, M., Wang, D., Du, L., Haddad, I. E., Slowik, J. G., and Prevot, A. S. H.: Uncovering the dominant contribution of intermediate volatility compounds in secondary organic aerosol formation from biomass-burning emissions, *Natl. Sci. Rev.*, 11, nwae014, <https://doi.org/10.1093/nsr/nwae014>, 2024.
- Li, X., Wang, S., Duan, L., Hao, J., Li, C., Chen, Y., and Yang, L.: Particulate and Trace Gas Emissions from Open Burning of Wheat Straw and Corn Stover in China, *Environ. Sci. Technol.*, 41, 6052–6058, <https://doi.org/10.1021/es0705137>, 2007.
- Li, Y., Pöschl, U., and Shiraiwa, M.: Molecular corridors and parameterizations of volatility in the chemical evolution of organic aerosols, *Atmos. Chem. Phys.*, 16, 3327–3344, <https://doi.org/10.5194/acp-16-3327-2016>, 2016.
- Li, Z., Wang, S., Li, S., Wang, X., Huang, G., Chang, X., Huang, L., Liang, C., Zhu, Y., Zheng, H., Song, Q., Wu, Q., Zhang, F., and Zhao, B.: High-resolution emission inventory of full-volatility organic compounds from cooking in China during 2015–2021, *Earth Syst. Sci. Data*, 15, 5017–5037, <https://doi.org/10.5194/essd-15-5017-2023>, 2023.
- Liu, C., Zhang, C., Mu, Y., Liu, J., and Zhang, Y.: Emission of volatile organic compounds from domestic coal stove with the actual alternation of flaming and smoldering combustion processes, *Environ. Pollut.*, 221, 385–391, <https://doi.org/10.1016/j.envpol.2016.11.089>, 2017.
- Liu, Y., Shao, M., Fu, L., Lu, S., Zeng, L., and Tang, D.: Source profiles of volatile organic compounds (VOCs) measured in China: Part I, *Atmos. Environ.*, 42, 6247–6260, <https://doi.org/10.1016/j.atmosenv.2008.01.070>, 2008.
- Liu, Y., Liao, B., Guo, W., Fu, Y., Sun, W., Fu, Y., Wang, D., and Kang, H.: Study on Separation and Purification of Chemical Components of Dichloromethane from Pine Needle Extract, *IOP C. Ser. Earth Env.*, 714, 032039, <https://doi.org/10.1088/1755-1315/714/3/032039>, 2021.
- Loebel Roson, M., Duruisseau-Kuntz, R., Wang, M., Klimchuk, K., Abel, R. J., Harynyuk, J. J., and Zhao, R.: Chemical Characterization of Emissions Arising from Solid Fuel Combustion – Contrasting Wood and Cow Dung Burning, *ACS Earth and Space Chemistry*, 5, 2925–2937, <https://doi.org/10.1021/acsearthspacechem.1c00268>, 2021.
- Ma, Y. and Hays, M. D.: Thermal extraction–two-dimensional gas chromatography–mass spectrometry with heart-cutting for nitrogen heterocyclics in biomass burning aerosols, *J. Chromatogr. A*, 1200, 228–234, 2008.
- Majluf, F. Y., Krechmer, J. E., Daube, C., Knighton, W. B., Dyroff, C., Lambe, A. T., Fortner, E. C., Yacovitch, T. I., Roscioli, J. R., Herndon, S. C., Worsnop, D. R., and Canagaratna, M. R.: Mobile Near-Field Measurements of Biomass Burning Volatile Organic Compounds: Emission Ratios and Factor Analysis, *Environ. Sci. Tech. Lett.*, 9, 383–390, <https://doi.org/10.1021/acs.estlett.2c00194>, 2022.
- Mann, H. B. and Whitney, D. R.: On a test of whether one of two random variables is stochastically larger than the other, *Ann. Math Stat.*, 18, 50–60, <https://doi.org/10.1214/aoms/1177730491>, 1947.
- Mastral, A. M. and Callen, M. S.: A review on polycyclic aromatic hydrocarbon (PAH) emissions from energy generation, *Environ. Sci. Technol.*, 34, 3051–3057, 2000.
- Nagai, K., Uranbileg, B., Chen, Z., Fujioka, A., Yamazaki, T., Matsumoto, Y., Tsukamoto, H., Ikeda, H., Yatomi, Y., and Chiba, H.: Identification of novel biomarkers of hepatocellular carcinoma by high-definition mass spectrometry: Ultrahigh-performance liquid chromatography quadrupole time-of-flight mass spectrometry and desorption electrospray ionization mass spectrometry imaging, *Rapid Commun. Mass Sp.*, 34, e8551, <https://doi.org/10.1002/rcm.8551>, 2020.
- Nelson Jr., R. M.: An evaluation of the carbon balance technique for estimating emission factors and fuel consumption, Research Paper SE-231, United States Department of Agriculture, Forest Service, Southeastern Forest Experiment Station, Asheville, NC, USA, 1982.
- Ni, H., Huang, R.-J., Pieber, S. M., Corbin, J. C., Stefenelli, G., Pospisilova, V., Klein, F., Gysel-Beer, M., Yang, L., and Baltensperger, U.: Brown carbon in primary and aged coal combustion emission, *Environ. Sci. Technol.*, 55, 5701–5710, 2021.
- Noe, S. M., Hüve, K., Niinemets, Ü., and Copolovici, L.: Seasonal variation in vertical volatile compounds air concentrations within a remote hemiboreal mixed forest, *Atmos. Chem. Phys.*, 12, 3909–3926, <https://doi.org/10.5194/acp-12-3909-2012>, 2012.
- Nomura, F., Tomonaga, T., Sogawa, K., Ohashi, T., Nezu, M., Sunaga, M., Kondo, N., Iyo, M., Shimada, H., and Ochiai, T.: Identification of novel and downregulated biomarkers for alcoholism by surface enhanced laser desorption/ionization-mass spectrometry, *Proteomics*, 4, 1187–1194, 2004.
- Oberschelp, C., Pfister, S., Raptis, C., and Hellweg, S.: Global emission hotspots of coal power generation, *Nat. Sustain.*, 2, 113–121, 2019.
- Permar, W., Wang, Q., Selimovic, V., Wielgasz, C., Yokelson, R. J., Hornbrook, R. S., Hills, A. J., Apel, E. C., Ku, I. T., and Zhou, Y.: Emissions of trace organic gases from Western US wildfires based on WE-CAN aircraft measurements, *J. Geophys. Res.-Atmos.*, 126, e2020JD033838, <https://doi.org/10.1029/2020JD033838>, 2021.
- Ren, Q. and Zhao, C.: Evolution of fuel-N in gas phase during biomass pyrolysis, *Renew. Sust. Energ. Rev.*, 50, 408–418, 2015.
- Riva, M., Rantala, P., Krechmer, J. E., Peräkylä, O., Zhang, Y., Heikkinen, L., Garmash, O., Yan, C., Kulmala, M., Worsnop, D., and Ehn, M.: Evaluating the performance of five different chemical ionization techniques for detecting gaseous oxygenated organic species, *Atmos. Meas. Tech.*, 12, 2403–2421, <https://doi.org/10.5194/amt-12-2403-2019>, 2019.
- Robinson, A. L., Donahue, N. M., Shrivastava, M. K., Weitkamp, E. A., Sage, A. M., Grieshop, A. P., Lane, T. E., Pierce, J. R., and Pandis, S. N.: Rethinking organic aerosols: Semivolatile emissions and photochemical aging, *Science*, 315, 1259–1262, 2007.
- Sarangi, B., Aggarwal, S. G., and Gupta, P. K.: Performance check of particle size standards within and after shelf-life using differential mobility analyzer, *J. Aerosol Sci.*, 103, 24–37, 2017.
- Sarkar, C., Sinha, V., Kumar, V., Rupakheti, M., Panday, A., Mahata, K. S., Rupakheti, D., Kathayat, B., and Lawrence, M. G.: Overview of VOC emissions and chemistry from PTR-TOF-MS measurements during the SusKat-ABC campaign: high acetaldehyde, isoprene and isocyanic acid in wintertime air of

- the Kathmandu Valley, *Atmos. Chem. Phys.*, 16, 3979–4003, <https://doi.org/10.5194/acp-16-3979-2016>, 2016.
- Schervish, M. and Donahue, N. M.: Peroxy radical chemistry and the volatility basis set, *Atmos. Chem. Phys.*, 20, 1183–1199, <https://doi.org/10.5194/acp-20-1183-2020>, 2020.
- Schneider, J., Weimer, S., Drewnick, F., Borrmann, S., Helas, G., Gwaze, P., Schmid, O., Andreae, M., and Kirchner, U.: Mass spectrometric analysis and aerodynamic properties of various types of combustion-related aerosol particles, *Int. J. Mass Spectrom.*, 258, 37–49, 2006.
- Sengpiel, R., Di Marino, D., Blindert, M., and Wessling, M.: 7 Hydroxotropic solutions for Fenton depolymerization of lignin, Extraction and Electrochemical Valorization of Lignin in Novel Electrolytes, 107, <https://doi.org/10.18154/RWTH-2019-09911>, 2019.
- Simoneit, B. R., Rogge, W., Mazurek, M., Standley, L., Hildemann, L., and Cass, G.: Lignin pyrolysis products, lignans, and resin acids as specific tracers of plant classes in emissions from biomass combustion, *Environ. Sci. Technol.*, 27, 2533–2541, 1993.
- Stala-Szlugaj, K.: The demand for hard coal for households in Poland and the anti-smog bill, *Arch. Min. Sci.*, 63, 701–711, 2018.
- Stewart, G. J., Acton, W. J. F., Nelson, B. S., Vaughan, A. R., Hopkins, J. R., Arya, R., Mondal, A., Jangirh, R., Ahlawat, S., Yadav, L., Sharma, S. K., Dunmore, R. E., Yunus, S. S. M., Hewitt, C. N., Nemitz, E., Mullinger, N., Gadi, R., Sahu, L. K., Tripathi, N., Rickard, A. R., Lee, J. D., Mandal, T. K., and Hamilton, J. F.: Emissions of non-methane volatile organic compounds from combustion of domestic fuels in Delhi, India, *Atmos. Chem. Phys.*, 21, 2383–2406, <https://doi.org/10.5194/acp-21-2383-2021>, 2021a.
- Stewart, G. J., Nelson, B. S., Acton, W. J. F., Vaughan, A. R., Farren, N. J., Hopkins, J. R., Ward, M. W., Swift, S. J., Arya, R., Mondal, A., Jangirh, R., Ahlawat, S., Yadav, L., Sharma, S. K., Yunus, S. S. M., Hewitt, C. N., Nemitz, E., Mullinger, N., Gadi, R., Sahu, L. K., Tripathi, N., Rickard, A. R., Lee, J. D., Mandal, T. K., and Hamilton, J. F.: Emissions of intermediate-volatility and semi-volatile organic compounds from domestic fuels used in Delhi, India, *Atmos. Chem. Phys.*, 21, 2407–2426, <https://doi.org/10.5194/acp-21-2407-2021>, 2021b.
- Stockwell, C. E., Veres, P. R., Williams, J., and Yokelson, R. J.: Characterization of biomass burning emissions from cooking fires, peat, crop residue, and other fuels with high-resolution proton-transfer-reaction time-of-flight mass spectrometry, *Atmos. Chem. Phys.*, 15, 845–865, <https://doi.org/10.5194/acp-15-845-2015>, 2015.
- Sun, Y., Chen, Y., Sun, C., Liu, H., Wang, Y., and Jiang, X.: Analysis of volatile organic compounds from patients and cell lines for the validation of lung cancer biomarkers by proton-transfer-reaction mass spectrometry, *Anal. Methods-UK*, 11, 3188–3197, 2019.
- Tao, S., Ru, M., Du, W., Zhu, X., Zhong, Q., Li, B., Shen, G., Pan, X., Meng, W., and Chen, Y.: Quantifying the rural residential energy transition in China from 1992 to 2012 through a representative national survey, *Nature Energy*, 3, 567–573, 2018.
- Teunissen, C., Koel-Simmelink, M., Pham, T., Knol, J., Khalil, M., Trentini, A., Killestein, J., Nielsen, J., Vrenken, H., and Popescu, V.: Identification of biomarkers for diagnosis and progression of MS by MALDI-TOF mass spectrometry, *Mult. Scler. J.*, 17, 838–850, 2011.
- Tkacik, D. S., Robinson, E. S., Ahern, A., Saleh, R., Stockwell, C., Veres, P., Simpson, I. J., Meinardi, S., Blake, D. R., Yokelson, R. J., Presto, A. A., Sullivan, R. C., Donahue, N. M., and Robinson, A. L.: A dual-chamber method for quantifying the effects of atmospheric perturbations on secondary organic aerosol formation from biomass burning emissions, *J. Geophys. Res.-Atmos.*, 122, 6043–6058, <https://doi.org/10.1002/2016jd025784>, 2017.
- Tong, Y., Pospisilova, V., Qi, L., Duan, J., Gu, Y., Kumar, V., Rai, P., Stefanelli, G., Wang, L., Wang, Y., Zhong, H., Baltensperger, U., Cao, J., Huang, R.-J., Prévôt, A. S. H., and Slowik, J. G.: Quantification of solid fuel combustion and aqueous chemistry contributions to secondary organic aerosol during wintertime haze events in Beijing, *Atmos. Chem. Phys.*, 21, 9859–9886, <https://doi.org/10.5194/acp-21-9859-2021>, 2021.
- Tritten, L., Keiser, J., Godejohann, M., Utzinger, J., Vargas, M., Beckonert, O., Holmes, E., and Saric, J.: Metabolic profiling framework for discovery of candidate diagnostic markers of malaria, *Sci. Rep.*, 3, 2769, <https://doi.org/10.1038/srep02769>, 2013.
- Wang, T.: Chemical characterization of organic vapors from wood, straw, cow dung, and coal burning, Zenodo [data set], <https://doi.org/10.5281/zenodo.14204573>, 2024.
- Wang, D. S., Lee, C. P., Krechmer, J. E., Majluf, F., Tong, Y., Canagaratna, M. R., Schmale, J., Prévôt, A. S. H., Baltensperger, U., Dommen, J., El Haddad, I., Slowik, J. G., and Bell, D. M.: Constraining the response factors of an extractive electrospray ionization mass spectrometer for near-molecular aerosol speciation, *Atmos. Meas. Tech.*, 14, 6955–6972, <https://doi.org/10.5194/amt-14-6955-2021>, 2021.
- Wang, T., Li, K., Bell, D. M., Zhang, J., Cui, T., Surdu, M., Baltensperger, U., Slowik, J. G., Lamkaddam, H., and El Haddad, I.: Large contribution of in-cloud production of secondary organic aerosol from biomass burning emissions, *npj Climate and Atmospheric Science*, 7, 149, <https://doi.org/10.1038/s41612-024-00682-6>, 2024.
- Warneke, C., Roberts, J. M., Veres, P., Gilman, J., Kuster, W. C., Burling, I., Yokelson, R., and de Gouw, J. A.: VOC identification and inter-comparison from laboratory biomass burning using PTR-MS and PIT-MS, *Int. J. Mass Spectrom.*, 303, 6–14, <https://doi.org/10.1016/j.ijms.2010.12.002>, 2011.
- Weber, K. T. and Yadav, R.: Spatiotemporal trends in wildfires across the Western United States (1950–2019), *Remote Sens.-Basel*, 12, 2959, <https://doi.org/10.3390/rs12182959>, 2020.
- Weimer, S., Alfara, M. R., Schreiber, D., Mohr, M., Prévôt, A. S. H., and Baltensperger, U.: Organic aerosol mass spectral signatures from wood-burning emissions: Influence of burning conditions and wood type, *J. Geophys. Res.*, 113, D10304, <https://doi.org/10.1029/2007jd009309>, 2008.
- White, R., Pulford, E., Elliot, D. J., Thurgood, L. A., and Klebe, S.: Quantitative mass spectrometry to identify protein markers for diagnosis of malignant pleural mesothelioma, *J. Proteomics*, 192, 374–382, 2019.
- Wiedensohler, A., Wiesner, A., Weinhold, K., Birmili, W., Hermann, M., Merkel, M., Müller, T., Pfeifer, S., Schmidt, A., and Tuch, T.: Mobility particle size spectrometers: Calibration procedures and measurement uncertainties, *Aerosol Sci. Technol.*, 52, 146–164, 2018.

- Wilcoxon, F.: Individual Comparisons by Ranking Methods, *Biometrics Bull.*, 1, 80–83, <https://doi.org/10.2307/3001968>, 1945.
- Williams, A. P., Allen, C. D., Macalady, A. K., Griffin, D., Woodhouse, C., Meko, D. M., Swetnam, T. W., Rauscher, S. A., Seager, R., and Grissino-Mayer, H. D.: Temperature as a potent driver of regional forest drought stress and tree mortality, *Nat. Clim. Change*, 3, 292–297, 2013.
- Wu, D., Zheng, H., Li, Q., Jin, L., Lyu, R., Ding, X., Huo, Y., Zhao, B., Jiang, J., and Chen, J.: Toxic potency-adjusted control of air pollution for solid fuel combustion, *Nature Energy*, 7, 194–202, 2022.
- Yuan, B., Koss, A. R., Warneke, C., Coggon, M., Sekimoto, K., and de Gouw, J. A.: Proton-Transfer-Reaction Mass Spectrometry: Applications in Atmospheric Sciences, *Chem. Rev.*, 117, 13187–13229, <https://doi.org/10.1021/acs.chemrev.7b00325>, 2017.
- Zhang, J. and Smith, K. R.: Household air pollution from coal and biomass fuels in China: measurements, health impacts, and interventions, *Environ. Health Perspect.*, 115, 848–855, 2007.
- Zhang, J., Smith, K., Ma, Y., Ye, S., Jiang, F., Qi, W., Liu, P., Khalil, M., Rasmussen, R., and Thorneloe, S.: Greenhouse gases and other airborne pollutants from household stoves in China: a database for emission factors, *Atmos. Environ.*, 34, 4537–4549, 2000.
- Zhang, J., Li, K., Wang, T., Gammelsæter, E., Cheung, R. K. Y., Surdu, M., Bogler, S., Bhattu, D., Wang, D. S., Cui, T., Qi, L., Lamkaddam, H., El Haddad, I., Slowik, J. G., Prevot, A. S. H., and Bell, D. M.: Bulk and molecular-level composition of primary organic aerosol from wood, straw, cow dung, and plastic burning, *Atmos. Chem. Phys.*, 23, 14561–14576, <https://doi.org/10.5194/acp-23-14561-2023>, 2023.
- Zhang, X., Xu, J., Zhai, L., and Zhao, W.: Characterization of Aerosol Properties from the Burning Emissions of Typical Residential Fuels on the Tibetan Plateau, *Environ. Sci. Technol.*, 56, 14296–14305, <https://doi.org/10.1021/acs.est.2c04211>, 2022.
- Zhao, B., Wang, S., Donahue, N. M., Jathar, S. H., Huang, X., Wu, W., Hao, J., and Robinson, A. L.: Quantifying the effect of organic aerosol aging and intermediate-volatility emissions on regional-scale aerosol pollution in China, *Sci. Rep.*, 6, 28815, <https://doi.org/10.1038/srep28815>, 2016.
- Zhao, N., Li, B., Ahmad, R., Ding, F., Zhou, Y., Li, G., Zayan, A. M. I., and Dong, R.: Dynamic relationships between real-time fuel moisture content and combustion-emission-performance characteristics of wood pellets in a top-lit updraft cookstove, *Case Studies in Thermal Engineering*, 28, 101484, <https://doi.org/10.1016/j.csite.2021.101484>, 2021.